The Plant Cell, Vol. 29: 1460–1479, June 2017, www.plantcell.org © 2017 ASPB.

Interplay of Plasma Membrane and Vacuolar Ion Channels, Together with BAK1, Elicits Rapid Cytosolic Calcium Elevations in Arabidopsis during Aphid Feeding[OPEN]

Thomas R. Vincent,[a] Marieta Avramova,[a] James Canham,[a] Peter Higgins,[b] Natasha Bilkey,[b,c] Sam T. Mugford,[b] Marco Pitino,[b] Masatsugu Toyota,[c,d,e] Simon Gilroy,[c] Anthony J. Miller,[a] Saskia A. Hogenhout,[b,1] and Dale Sanders[a,1]

[a] Department of Metabolic Biology, John Innes Centre, Norwich NR4 7UH, United Kingdom
[b] Department of Crop Genetics, John Innes Centre, Norwich NR4 7UH, United Kingdom
[c] Department of Botany, University of Wisconsin, Madison, Wisconsin 53706
[d] Department of Biochemistry and Molecular Biology, Saitama University, Sakura-ku, Saitama 338-8570, Japan
[e] Japan Science and Technology Agency, Precursory Research for Embryonic Science and Technology (PRESTO), Kawaguchi, Saitama 332-0012, Japan

ORCID IDs: 0000-0001-9597-6839 (S.G.); 0000-0003-0572-7607 (A.J.M.); 0000-0003-1371-5606 (S.A.H.); 0000-0002-1452-9808 (D.S.)

A transient rise in cytosolic calcium ion concentration is one of the main signals used by plants in perception of their environment. The role of calcium in the detection of abiotic stress is well documented; however, its role during biotic interactions remains unclear. Here, we use a fluorescent calcium biosensor (GCaMP3) in combination with the green peach aphid (*Myzus persicae*) as a tool to study *Arabidopsis thaliana* calcium dynamics in vivo and in real time during a live biotic interaction. We demonstrate rapid and highly localized plant calcium elevations around the feeding sites of *M. persicae*, and by monitoring aphid feeding behavior electrophysiologically, we demonstrate that these elevations correlate with aphid probing of epidermal and mesophyll cells. Furthermore, we dissect the molecular mechanisms involved, showing that interplay between the plant defense coreceptor BRASSINOSTEROID INSENSITIVE-ASSOCIATED KINASE1 (BAK1), the plasma membrane ion channels GLUTAMATE RECEPTOR-LIKE 3.3 and 3.6 (GLR3.3 and GLR3.6), and the vacuolar ion channel TWO-PORE CHANNEL1 (TPC1) mediate these calcium elevations. Consequently, we identify a link between plant perception of biotic threats by BAK1, cellular calcium entry mediated by GLRs, and intracellular calcium release by TPC1 during a biologically relevant interaction.

INTRODUCTION

Transient rises in cytosolic calcium ion concentration ($[Ca^{2+}]_{cyt}$) act as ubiquitous signals that coordinate a range of physiological processes in plants. The capacity for abiotic stresses such as cold, salt, and drought to elicit $[Ca^{2+}]_{cyt}$ elevations in plants has been known for some time (Knight et al., 1991; McAinsh et al., 1995; Allen et al., 2000; Kiegle et al., 2000). Biotic stresses such as plant pathogens can also elicit $[Ca^{2+}]_{cyt}$ elevations; however, the study of these elevations has been largely restricted to the use of elicitors as opposed to live organisms (Blume et al., 2000; Lecourieux et al., 2005; Thor and Peiter, 2014; Keinath et al., 2015; Charpentier et al., 2016). Conversely, although application of live chewing insects elicits large $[Ca^{2+}]_{cyt}$ elevations, these are hard to differentiate from those caused by wounding alone (Verrillo et al., 2014; Kiep et al., 2015). The green peach aphid (*Myzus persicae*), which pierces a small number of plant cells (Will and van Bel, 2006), offers a unique opportunity to study plant Ca^{2+} dynamics in vivo during a biotic stress more akin to plant-microbe interactions.

Plants perceive detrimental biotic events through the detection of conserved pathogen-associated molecular patterns (PAMPs)/herbivore-associated molecular patterns, by pathogen recognition receptors (PRRs) in the plant (Chinchilla et al., 2006; Zipfel et al., 2006; Yamaguchi et al., 2006; Miya et al., 2007), many of which interact with the defense coreceptor BRASSINOSTEROID INSENSITIVE1-ASSOCIATED KINASE1 (BAK1) (Chinchilla et al., 2007; Heese et al., 2007) during response known as PAMP-triggered immunity (PTI) (Jones and Dangl, 2006; Zipfel, 2009; Mithöfer and Boland, 2008). One of the earliest events upon pathogen recognition is a transient elevation in $[Ca^{2+}]_{cyt}$ (Blume et al., 2000; Lecourieux et al., 2005; Keinath et al., 2015), while a hallmark of symbiotic biotic interactions is $[Ca^{2+}]$ oscillations in the nucleus (Ehrhardt et al., 1996; Kosuta et al., 2008). Despite this, the mechanisms underlying $[Ca^{2+}]_{cyt}$ elevations during biotic interactions have remained unclear, although several Ca^{2+}-permeable channels have been suggested to play a role. The CYCLIC NUCLEOTIDE GATED CHANNEL (CNGC) and GLUTAMATE RECEPTOR-LIKE CHANNEL (GLR) families include some of the best-characterized plasma membrane Ca^{2+}-permeable channel families in plants (Dodd et al., 2010). CNGC15 facilitates nuclear $[Ca^{2+}]$ oscillations in response to symbiotic elicitors (Charpentier et al., 2016), while CNCG2 mediates entry of Ca^{2+} from the apoplast (Wang et al., 2017) and the *CNGC2*-null mutant *defense no death1* exhibits a constitutive defense phenotype (Yu et al., 1998; Clough et al., 2000). Furthermore, *GLR3.3* and *GLR3.6* have been implicated in

[1] Address correspondence to saskia.hogenhout@jic.ac.uk or dale.sanders@jic.ac.uk.
The author responsible for distribution of materials integral to the findings presented in this article in accordance with the policy described in the Instructions for Authors (www.plantcell.org) is: Dale Sanders (dale.sanders@jic.ac.uk).
[OPEN]Articles can be viewed without a subscription.
www.plantcell.org/cgi/doi/10.1105/tpc.17.00136

systemic signaling during wounding (Mousavi et al., 2013; Salvador-Recatalà, 2016). In addition, herbivory-elicited Ca^{2+} signals are attenuated in null mutants of the vacuolar channel *TWO-PORE CHANNEL1* (*TPC1*) (Kiep et al., 2015). TPC1 is a tonoplast-localized Ca^{2+}-permeable channel whose activity is regulated by voltage and Ca^{2+} (Hedrich and Neher, 1987; Ward and Schroeder, 1994; Peiter et al., 2005; Gradogna et al., 2009; Guo et al., 2016, 2017; Kintzer and Stroud, 2016). TPC1 also has an established role in systemic Ca^{2+} signaling in response to salt stress (Choi et al., 2014; Evans et al., 2016) and wounding (Kiep et al., 2015) via its positive regulation by Ca^{2+} in a process termed Ca^{2+}-induced Ca^{2+} release. However, the mechanism by which Ca^{2+}-induced Ca^{2+} release is triggered in plants remains unknown.

M. persicae is a significant agricultural pest due to its highly polyphagous nature (Blackman and Eastop, 2000; Schoonhoven et al., 2005; Blackman and Eastop, 2007; Mathers et al., 2017). Aphids pierce plant tissue using specialized mouthparts, called stylets, to establish long-term feeding from the phloem (Dixon, 1998). On the route to the phloem, the stylets navigate between epidermal and mesophyll cells, occasionally penetrating these cells during a process known as the pathway feeding phase (Tjallingii, 1985; Tjallingii and Esch, 1993). The ability of an aphid to feed successfully on a plant appears to be partly determined during these penetrations, as the pathway phase still occurs with aphid species unable to establish long-term feeding (Chen et al., 1997; Sauge et al., 1998; Jaouannet et al., 2015; Nam and Hardie, 2012). Furthermore, as with microbial pathogens, aphids are detected through a BAK1-dependent mechanism, although the PRRs involved have remained elusive, with FLAGELLIN-SENSITIVE2 (FLS2), EF-TU RECEPTOR (EFR), CHITIN ELICITOR RECEPTOR KINASE1 (CERK1), PEP1 RECEPTOR1 (PEPR1), and PEPR2 not appearing to play a role (Prince et al., 2014; Chaudhary et al., 2014).

There is circumstantial evidence that Ca^{2+} signaling is relevant to plant-aphid interactions. The majority of plant gene expression studies performed after infestation with aphids reveal a significant overrepresentation of Ca^{2+} signaling-related transcripts, most of which display upregulation (Foyer et al., 2015). In addition, feeding by *M. persicae* elicits plasma membrane depolarizations in *Arabidopsis thaliana* mesophyll cells (Bricchi et al., 2012), and Ca^{2+}-selective microelectrodes detect a significant Ca^{2+} flux out of the extracellular space into tobacco (*Nicotiana tabacum*) mesophyll cells after infestation with *M. persicae* (Ren et al., 2014). However, the primary role of Ca^{2+} in plant-aphid interactions is believed to be in the phloem, where it is hypothesized to have a function in signaling by promoting occlusion via regulation of callose production (Kauss et al., 1983; Singh and Paolillo, 1990; Aidemark et al., 2009) and plugging by phloem proteins (Knoblauch et al., 2001, 2003; Furch et al., 2009). Furthermore, it has been suggested that proteins in aphid saliva act to chelate phloem Ca^{2+} to prevent occlusion. Indeed, aphid saliva contains Ca^{2+} binding proteins (Will et al., 2007; Carolan et al., 2009; Rao et al., 2013), and application of saliva to legume phloem-plugging proteins results in their contraction (Will et al., 2007). Aphid saliva also contains effector molecules that suppress plant defense (Bos et al., 2010; Pitino and Hogenhout, 2013; Atamian et al., 2013; Naessens et al., 2015; Wang et al., 2015; Kettles and Kaloshian, 2016), as observed with microbial pathogens (Jones and Dangl, 2006; Galán et al., 2014) and chewing insects (Musser et al., 2002).

To date, there have been no direct measurements of local $[Ca^{2+}]_{cyt}$ dynamics in a leaf when only a few cells are under biotic attack. Aphids offer an approach by which to study such dynamics because the stylets of these insects probe individual plant cells, and this behavior can be monitored electrophysiologically (Tjallingii, 1985; Tjallingii and Esch, 1993). Here, using transgenic Arabidopsis plants expressing the GFP-based Ca^{2+} sensor GCaMP3 (Tian et al., 2009), we were able to show that aphid probing of epidermal and mesophyll cells elicits rapid and highly localized $[Ca^{2+}]_{cyt}$ elevations around aphid-feeding sites. We found that these $[Ca^{2+}]_{cyt}$ elevations depend on *BAK1*, *GLR3.3*/*GLR3.6*, and *TPC1*, indicating that $[Ca^{2+}]_{cyt}$ is produced as part of a cellular PTI response and is then propagated via the influx of extracellular and vacuolar Ca^{2+} and interplay between Ca^{2+}-permeable channels.

RESULTS

Aphids Elicit Rapid and Highly Localized $[Ca^{2+}]_{cyt}$ Elevations in Arabidopsis

Although other single wavelength Ca^{2+} sensors have been used in plants, including Case12 (Zhu et al., 2010) and RGECO (Keinath et al., 2015), we chose to apply GCaMP3, a Ca^{2+}-responsive probe that combines a large dynamic range, photostability, and compatibility with standard GFP-based imaging equipment (Tian et al., 2009). In addition, the assay for imaging calcium dynamics around aphid feeding requires relatively low magnification to capture the final feeding site selected by the insect without disturbing (moving) the sample. We have found the ease of detection and compatibility with the stereofluorescence microscopy makes this probe superior for these assays when compared with, e.g., the ratiometric yellow cameleon Ca^{2+} sensors (e.g., Choi et al., 2014) that need more sophisticated ratio imaging equipment such as a confocal microscope for accurate quantification.

To assess whether $[Ca^{2+}]_{cyt}$ elevations are seen in *35S:GCaMP3* Arabidopsis plants during *M. persicae* feeding, a single leaf assay was developed. This assay was set up by detaching leaves from *35S:GCaMP3* plants and floating leaves on water inside single wells of a 96-well plate. Because wounding induces Ca^{2+} signals in leaves (Kiep et al., 2015), the single leaves were detached and placed into plates 24 h prior to the start of microscopy experiments to allow wound-induced Ca^{2+} signals to dissipate. The floating leaf assay prevented aphid escape from the wells and allowed standardization of the assay by restricting aphid feeding to the abaxial surface of leaves of similar developmental stages.

Upon transferring a *M. persicae* individual to a *35S:GCaMP3* leaf, a clear increase in GCaMP3 (GFP) fluorescence was observed around the feeding site (Figure 1A; Supplemental Movie 1), which indicated a rise in $[Ca^{2+}]_{cyt}$ (Tian et al., 2009). This rise was consistent and significantly greater than the fluorescence in equivalent locations on no-aphid control leaves (Figure 1B). Typically, the fluorescence burst was generated

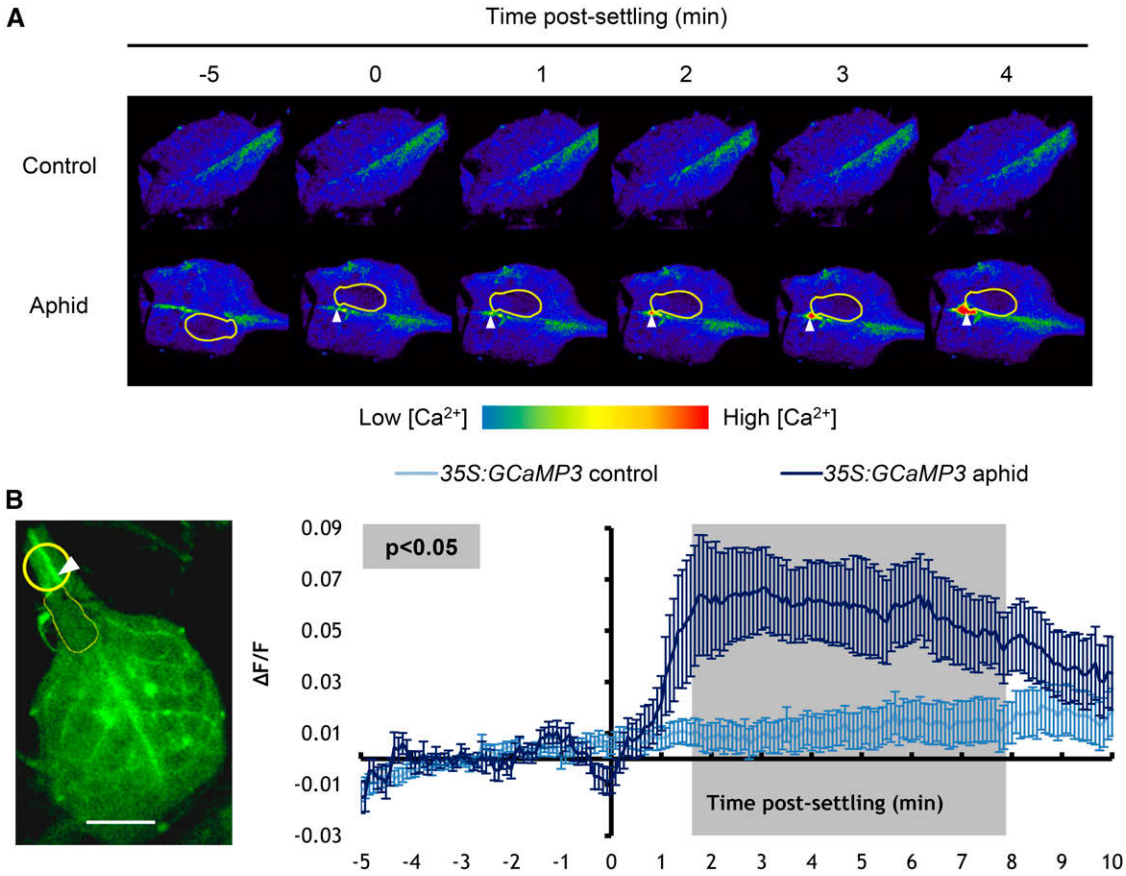

Figure 1. The GCaMP3 Sensor Detects $[Ca^{2+}]_{cyt}$ Elevations around the Aphid Feeding Site on Detached Leaves.

(A) Representative stereomicroscope images showing GFP fluorescence (color-coded according to the inset scale) around feeding sites of leaves exposed to a *M. persicae* adult at several time points after aphid settling. Aphid is outlined in yellow. Location of feeding site indicated with an arrowhead.
(B) Left: Stereomicroscope image of a feeding site region (yellow circle) used for the analyses shown on the right (bar = 1 mm). Aphid is outlined in yellow, and location of feeding site is indicated with an arrowhead. Right: Normalized GFP fluorescence (ΔF/F) measurements every 5 s around the feeding site from 5 min before until 10 min after settling of an adult aphid. F, average fluorescence intensity prior to aphid settling (baseline); ΔF, difference between measured fluorescence and baseline fluorescence. Error bars represent the SE of the mean ($n = 34$). The average area of the $[Ca^{2+}]_{cyt}$ elevation was 110 ± 18 μm^2, and the leading wave front of this elevation traveled radially at 5.9 ± 0.6 μm/s from its center. Gray shading indicates a significant difference between treatments using a Student's *t* test within a GLM at $P < 0.05$.

within 95 s upon settling of the aphids (Figure 1B; Supplemental Movie 1), with settling defined as an aphid remaining stationary for 5 min. From a total of 33 observations, the average area of the $[Ca^{2+}]_{cyt}$ elevation was 110 ± 18 μm^2 and the leading wave front of this elevation traveled radially at 5.9 ± 0.6 μm/s from its center. Although variation in the raw GFP fluorescence (F) could be observed between leaves under the microscope (e.g., Supplemental Movie 1; Figure 1A), for quantitative analysis this was accounted for by normalizing the GFP fluorescence to the baseline fluorescence before the aphid settled (ΔF/F, Figure 1B).

The aphid-elicited increase in fluorescence was not detected in regions of the leaf systemic to the feeding site (Figure 2). It has been shown previously that it is possible to detect systemic $[Ca^{2+}]_{cyt}$ elevations in detached leaves in response to salt stress (Xiong et al., 2014), suggesting that detachment of leaves does not prohibit the detection of systemic signals. Furthermore, whole plants exposed to aphids also exhibited $[Ca^{2+}]_{cyt}$ elevations, although a high number of replicates was not possible as it proved to be challenging to track aphid movement on a whole plant (Supplemental Movie 2). By contrast, the detached leaf assay was capable of detecting changes in $[Ca^{2+}]_{cyt}$ around the aphid-feeding site in a robust and repeatable manner. Indeed, confocal microscopy confirmed that GCaMP fluorescence was present primarily in the cytosol and not within the vacuole, although the presence of the GCAMP3 sensor within the nucleus could not be excluded (Supplemental Figure 1).

Aphid-Induced $[Ca^{2+}]_{cyt}$ Elevations Occur during Probing of the Epidermal and Mesophyll Cells

To investigate where the aphid stylets induce plant $[Ca^{2+}]_{cyt}$ elevations, the aphid stylet behavior was monitored using the electrical penetration graph (EPG) technique (Tjallingii, 1978; Salvador-Recatala and Tjallingii, 2015). In this technique, the stylet

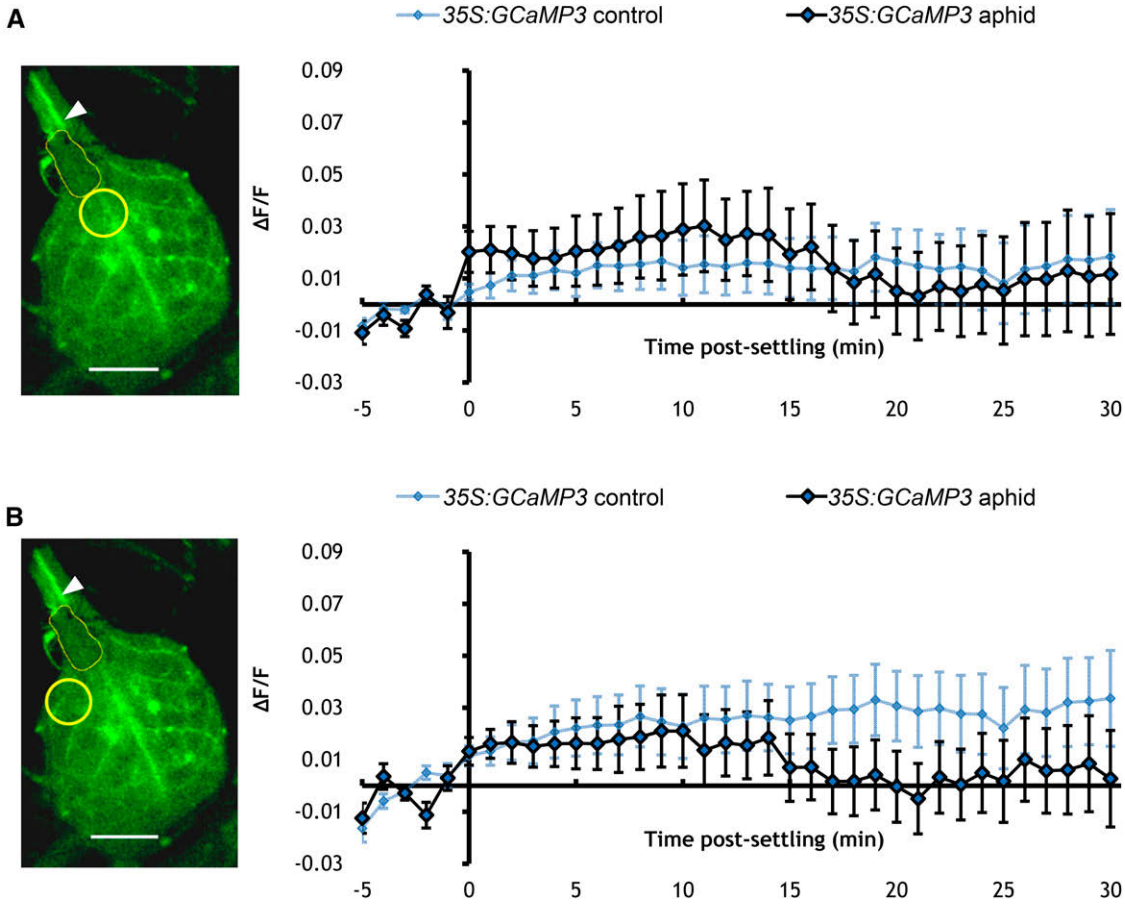

Figure 2. The GCaMP3 Sensor Does Not Detect $[Ca^{2+}]_{cyt}$ Elevations Systemic to the Aphid-Feeding Site.

(A) Left: Stereomicroscope image of a leaf exposed to an aphid with the yellow circle indicating the midrib region systemic to the feeding site (arrowhead) of an aphid (outlined in yellow). Bar = 1 mm. Right: Normalized fluorescence (ΔF/F) at midrib regions systemic to the aphid feeding sites (as exemplified with the yellow circle in the image on the left) of *35S:GCaMP3* leaves exposed to *M. persicae* adults and no-aphid controls. Error bars represent SE of the mean ($n = 34$). Data from aphid responding leaves are not significantly different from controls (Student's *t* test within a GLM, $P > 0.05$).

(B) Left: Stereomicroscope image of a leaf exposed to an aphid with the yellow circle indicating the lateral tissue regions (next to the midrib) systemic to the feeding site (arrowhead) of an aphid (outlined in yellow). Right: ΔF/F at lateral tissue regions systemic to the aphid-feeding sites (as exemplified with the yellow circle in the image on the left) of *35S:GCaMP3* leaves exposed to *M. persicae* adults and no-aphid controls. Error bars represent SE of the mean ($n = 34$). Data from aphid responding leaves are not significantly different from controls (Student's *t* test within a GLM, $P > 0.05$).

penetrations of epidermal and mesophyll cells during the pathway phase versus the phloem feeding phase can be monitored as distinct changes in voltage output (Figure 3). From 22 observations on soil-grown plants, the first cell punctures occurred at 31 ± 11 s after the beginning of the pathway phase, with the phloem being accessed after 24 ± 3 min (Figure 3A). An adapted version of the EPG technique to assess feeding behavior on detached *35S:GCaMP3* leaves floating in water showed that the timing of the pathway and phloem feeding phases of aphids on detached *35S:GCaMP3* leaves were comparable to those of soil-grown Col-0 plants, with the pathway phase lasting for 15 to 25 min (Figure 3B). In both EPG assays, the pathway phases began very rapidly upon aphid settling (Figure 3) and within the time frame of the aphid-induced $[Ca^{2+}]_{cyt}$ elevation (Figure 1B). Thus, the aphid-induced $[Ca^{2+}]_{cyt}$ elevations mostly likely occur during the pathway phase when the aphid stylets probe epidermal and mesophyll cells.

Ca^{2+} is hypothesized to play a role in the phloem during plant-aphid interactions (Will et al., 2007). To investigate whether an aphid-elicited $[Ca^{2+}]_{cyt}$ elevation occurs in the phloem, the GCaMP3 sensor was expressed under control of the *SUCROSE-PROTON SYMPORTER2* (*SUC2pro*) promoter (Stadler and Sauer, 1996). In contrast to the *35S:GCaMP3* leaves, *SUC2pro:GCaMP3* leaves did not show aphid-elicited $[Ca^{2+}]_{cyt}$ elevations, though there was a gradual increase in fluorescence over time that occurred independently of the presence of aphids (Figure 4; Supplemental Movie 3). In addition, cold shock is a well-characterized elicitor of Ca^{2+} signals in plants (Knight et al., 1996; Knight and Knight, 2000; Kiegle et al., 2000). Therefore, to confirm that the *SUC2pro:GCaMP3* construct was capable of reporting changes in phloem Ca^{2+} dynamics, *SUC2pro:GCaMP3* leaves were treated with cold water (Knight et al., 1996; Knight and Knight, 2000; Kiegle et al., 2000) and showed a clear increase in

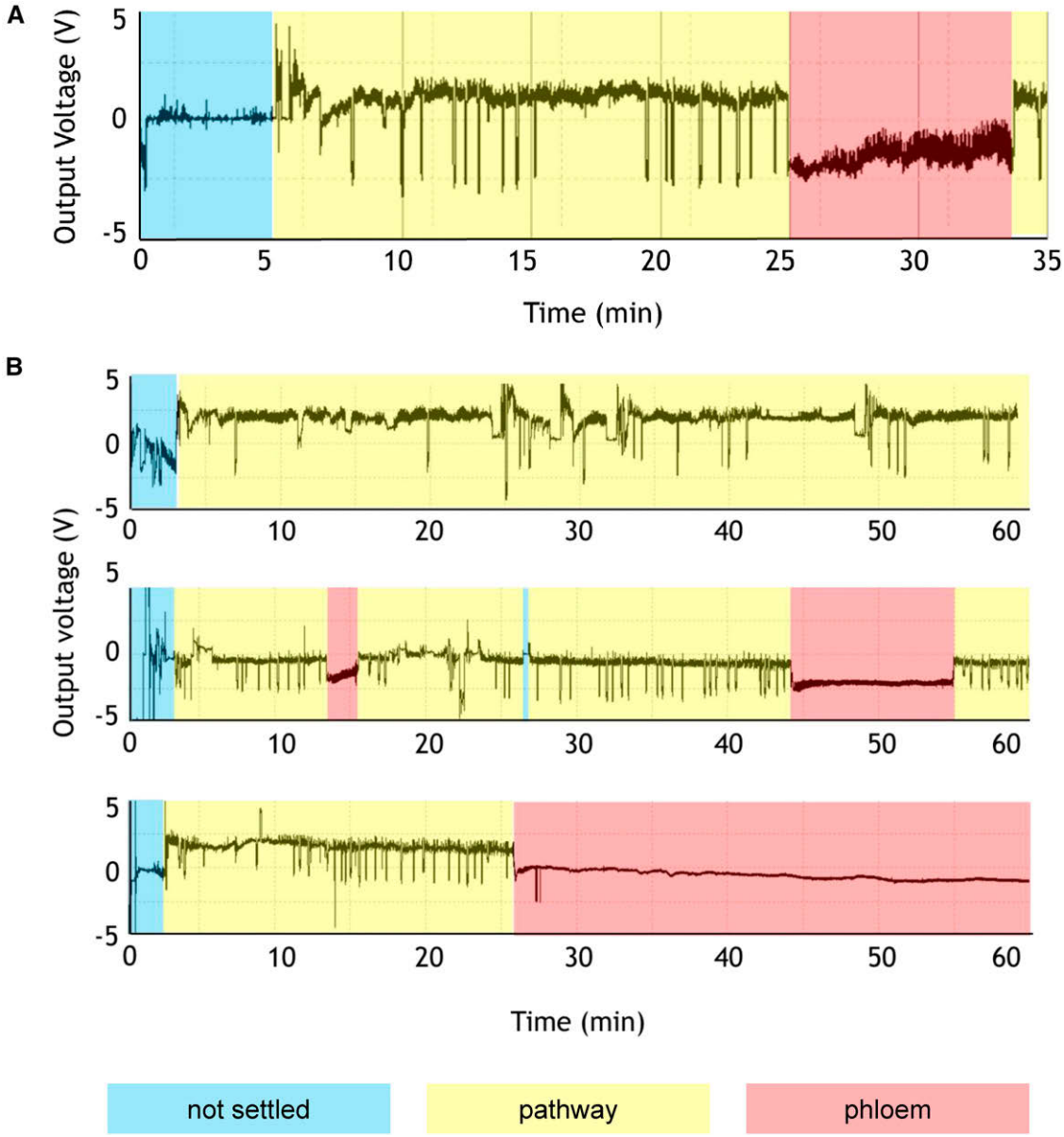

Figure 3. The Pathway Phase That Includes Aphid Probing of Epidermal and Mesophyll Cells Starts Immediately upon Aphid Settling.

Feeding phases are represented by colored shading.
(A) Representative EPG trace from an aphid feeding on a whole Col-0 Arabidopsis plant. The first cell puncture occurred at 31 ± 11 s after the beginning of pathway phase, with the phloem accessed after 24 ± 3 min (n = 22).
(B) Representative EPG traces from aphids feeding on detached *35S:GCaMP3* leaves (n = 6).

GFP fluorescence (Supplemental Movie 4). Thus, it does not appear that *M. persicae* elicits $[Ca^{2+}]_{cyt}$ elevations in the Arabidopsis phloem.

Aphid Elicitation of $[Ca^{2+}]_{cyt}$ Is Dependent on BAK1 and GLR3.3/GLR3.6

BAK1 is a defense coreceptor required for PTI against microbes (Chinchilla et al., 2007; Heese et al., 2007) and aphids (Prince et al., 2014; Chaudhary et al., 2014). Thus, to establish whether the aphid-elicited $[Ca^{2+}]_{cyt}$ elevation is a component of PTI, *35S:GCaMP3*-expressing plants were crossed with the *BAK1* null mutant *bak1-5*. The *bak1-5* mutant was selected as it displays defects in immune signaling, but not in brassinosteroid signaling as seen with other *BAK1* mutants (Schwessinger et al., 2011). Whereas *35S:GCaMP3* leaves exhibited the characteristic $[Ca^{2+}]_{cyt}$ elevations around aphid-feeding site (Figure 5A), these $[Ca^{2+}]_{cyt}$

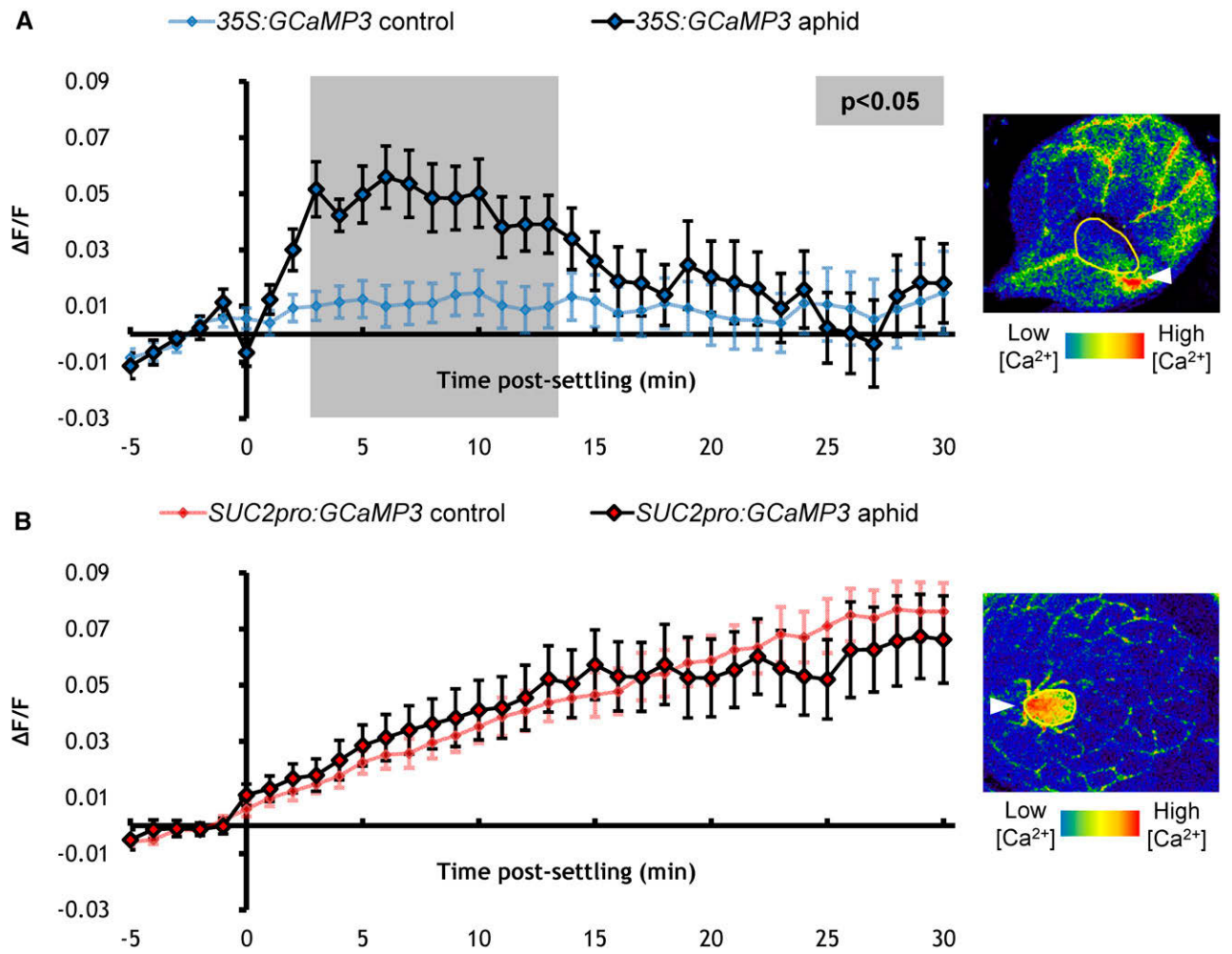

Figure 4. $[Ca^{2+}]_{cyt}$ Elevations Are Not Detected in the Phloem around Aphid-Feeding Sites.

(A) Left: Normalized fluorescence (ΔF/F) around aphid-feeding sites of *35S:GCaMP3* aphid-exposed leaves and no-aphid controls. Error bars represent SE of the mean (n = 31). Gray shading indicates significant difference between treatments (Student's t test within GLM at $P < 0.05$). Right: Representative stereomicroscope image of a $[Ca^{2+}]_{cyt}$ elevation seen around an aphid-feeding site on a *35S:GCaMP3* leaf. GFP fluorescence is color-coded according to the inset scale. Aphid outlined in yellow and feeding site indicated with an arrowhead. Image taken at 3 min after settling.

(B) Left: ΔF/F around the aphid-feeding sites of *SUC2pro:GCaMP3* aphid-exposed leaves and no-aphid controls. Error bars represent SE of the mean (n = 34). Right: Representative stereomicroscope image of the absence of $[Ca^{2+}]_{cyt}$ elevation around an aphid-feeding site on a *SUC2pro:GCaMP3* leaf. GFP fluorescence is color-coded according to the inset scale. Aphid outlined in yellow and feeding site indicated with an arrowhead. Image taken at 3 min after settling.

elevations were abolished in leaves of *35S:GCaMP3* x *bak1-5* line (Figures 5B and 5C; Supplemental Movie 5). Thus, BAK1 is required for inducing $[Ca^{2+}]_{cyt}$ elevations around aphid-feeding sites.

The plasma membrane cation-permeable channels *GLR3.3* and *GLR3.6* have recently been implicated in the Arabidopsis wound response, with systemic electrical signals migrating via the phloem being attenuated in the *GLR* double mutant *glr3.3 glr3.6* (Mousavi et al., 2013). To investigate if these channels also have a role in the more local systemic spread around the aphid-feeding sites, we generated a *35S:GCaMP3* × *glr3.3 glr3.6* line. The aphid-induced $[Ca^{2+}]_{cyt}$ elevation was also abolished in this line (Figure 6; Supplemental Movie 6). These data indicate that *GLR3.3* and *GLR3.6* are required for inducing $[Ca^{2+}]_{cyt}$ elevations around aphid-feeding sites.

TPC1 Contributes to the Aphid-Elicited $[Ca^{2+}]_{cyt}$ Elevation

TPC1 has been implicated in Ca^{2+} signaling during insect attack, with local and systemic wound-induced Ca^{2+} signals lost in the *tpc1-2* mutant (Kiep et al., 2015). To assess whether *TPC1* plays a role in aphid-induced Ca^{2+} signaling, GCaMP3 was introduced into the *tpc1-2* mutant and the *35S:TPC1 5.6* overexpression line (Peiter et al., 2005). In comparison to *35S:GCaMP3* (Figure 7A), the $[Ca^{2+}]_{cyt}$ elevations around the aphid-feeding sites of *35S:GCaMP3* x *tpc1-2* leaves were significantly reduced, though not totally abolished (Figures

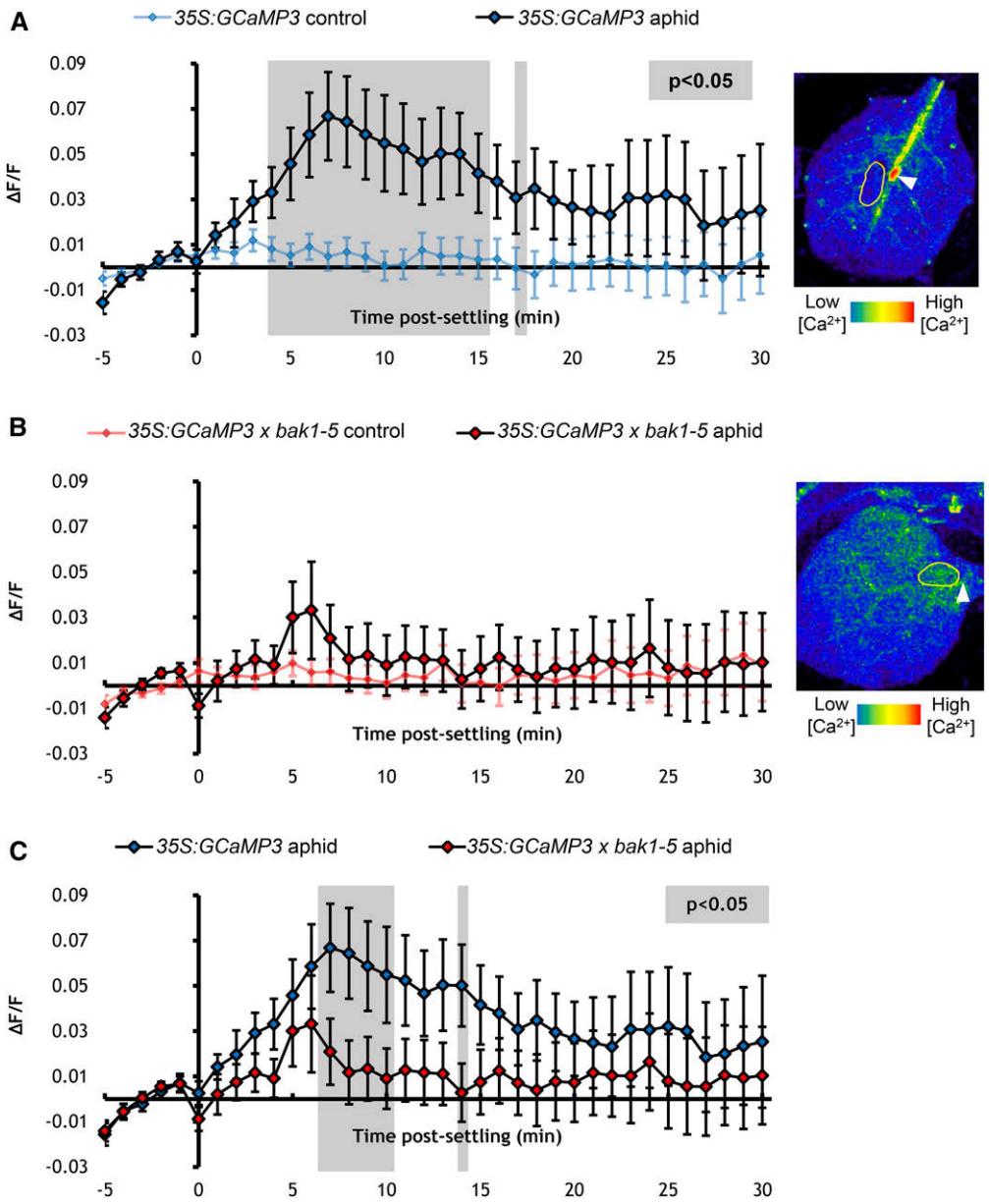

Figure 5. *BAK1* Is Required for Eliciting $[Ca^{2+}]_{cyt}$ Elevations around Aphid-Feeding Sites.

(A) Left: Normalized fluorescence (ΔF/F) around feeding sites of *35S:GCaMP3* aphid-exposed leaves and no-aphid controls. Error bars represent SE of the mean (n = 30). Gray shading indicates significant difference between treatments (Student's t test within GLM at $P < 0.05$). Right: Representative stereomicroscope image of the $[Ca^{2+}]_{cyt}$ elevation seen around an aphid-feeding site of a *35S:GCaMP3* leaf. GFP fluorescence color-coded according to the inset scale. Aphid outlined in yellow and feeding site indicated with an arrowhead. Image taken at 2 min after settling

(B) Left: ΔF/F around feeding sites of *35S:GCaMP3* × *bak1-5* aphid-exposed leaves and no-aphid controls. Error bars represent SE of the mean (n = 34). Right: Representative stereomicroscope image of the absence of $[Ca^{2+}]_{cyt}$ elevation around an aphid-feeding site of a *35S:GCaMP3* × *bak1-5* leaf. GFP fluorescence color-coded according to the inset scale. Aphid outlined in yellow and feeding site indicated with an arrowhead. Image taken at 2 min after settling.

(C) Comparison of ΔF/F around feeding sites of aphid-exposed *35S:GCaMP3* and *35S:GCaMP3* × *bak1-5* leaves. Data of aphid exposures shown in **(A)** and **(B)** were replotted together. Areas shaded in gray indicate significant differences between the two treatments (Student's t test within GLM at $P < 0.05$).

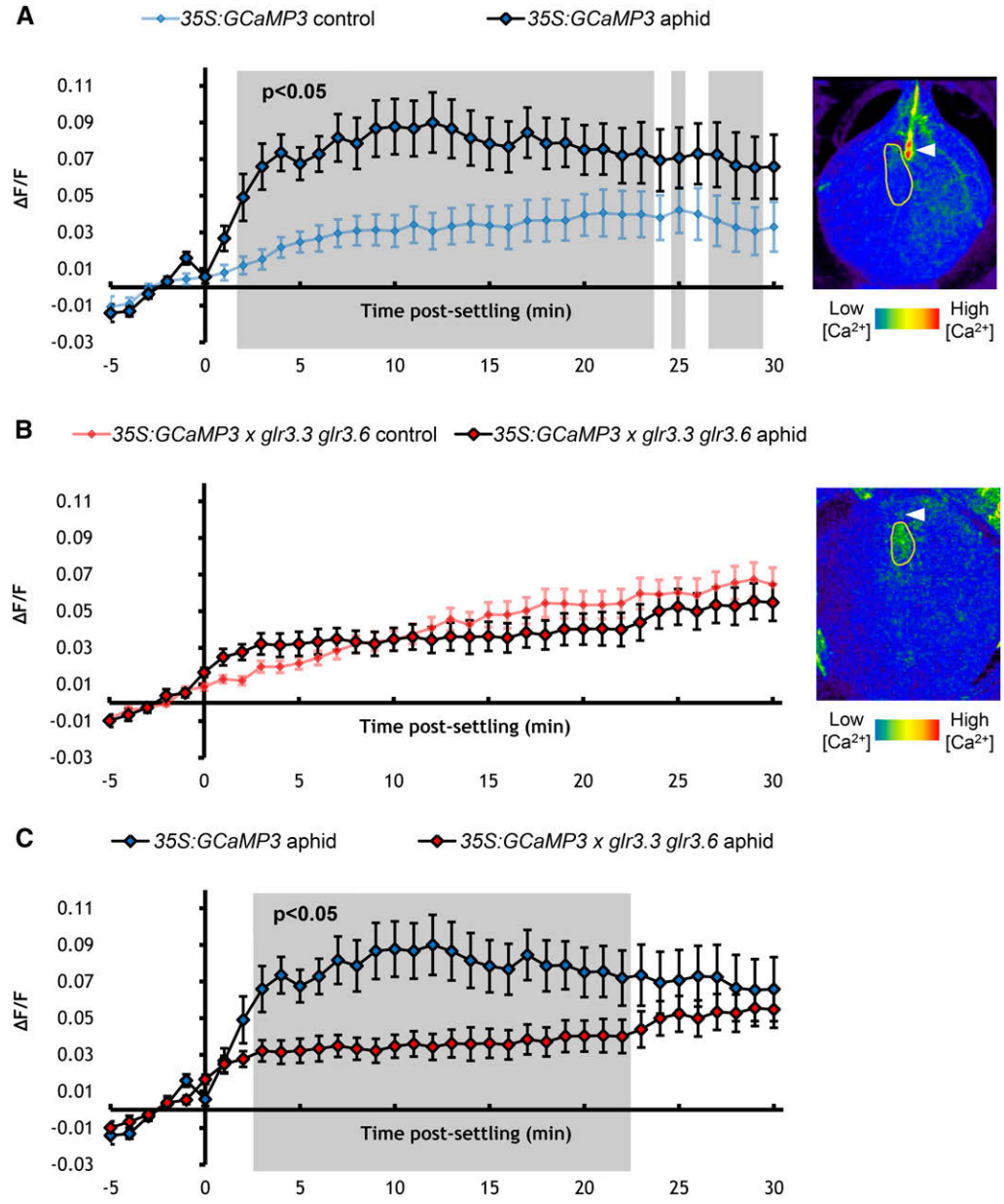

Figure 6. *GLR3.3* and *GLR3.6* Are Required for $[Ca^{2+}]_{cyt}$ Elevations Elicited around Aphid-Feeding Sites.

(A) Left: Normalized fluorescence (ΔF/F) around feeding sites of *35S:GCaMP3* aphid-exposed leaves and no-aphid controls. Error bars represent SE of the mean (n = 34). Gray shading indicates significant difference between treatments (Student's t test within GLM at P < 0.05). Right: Representative stereomicroscope image of the $[Ca^{2+}]_{cyt}$ elevations seen around an aphid-feeding site of a *35S:GCaMP3* leaf. GFP fluorescence is color-coded according to the inset scale. Aphid outlined in yellow and feeding site indicated with an arrowhead. Image taken at 3 min after settling.

(B) Left: ΔF/F around feeding sites of *35S:GCaMP3* × *glr3.3 glr3.6* aphid-exposed leaves and no-aphid controls. Error bars represent SE of the mean (n = 37). Right: Representative stereomicroscope image of the absence $[Ca^{2+}]_{cyt}$ elevation around an aphid-feeding site of a *35S:GCaMP3* × *glr3.3 3.6* leaf. GFP fluorescence is color-coded according to the inset scale. Aphid outlined in yellow and feeding site indicated with an arrowhead. Image taken at 3 min after settling.

(C) Comparison of ΔF/F around feeding sites of aphid-exposed *35S:GCaMP3* and *35S:GCaMP3* × *glr3.3 glr3.6* leaves. Data of aphid exposures shown in **(A)** and **(B)** were replotted together. Areas shaded in gray indicate significant differences between the two treatments (Student's t test within GLM at P < 0.05).

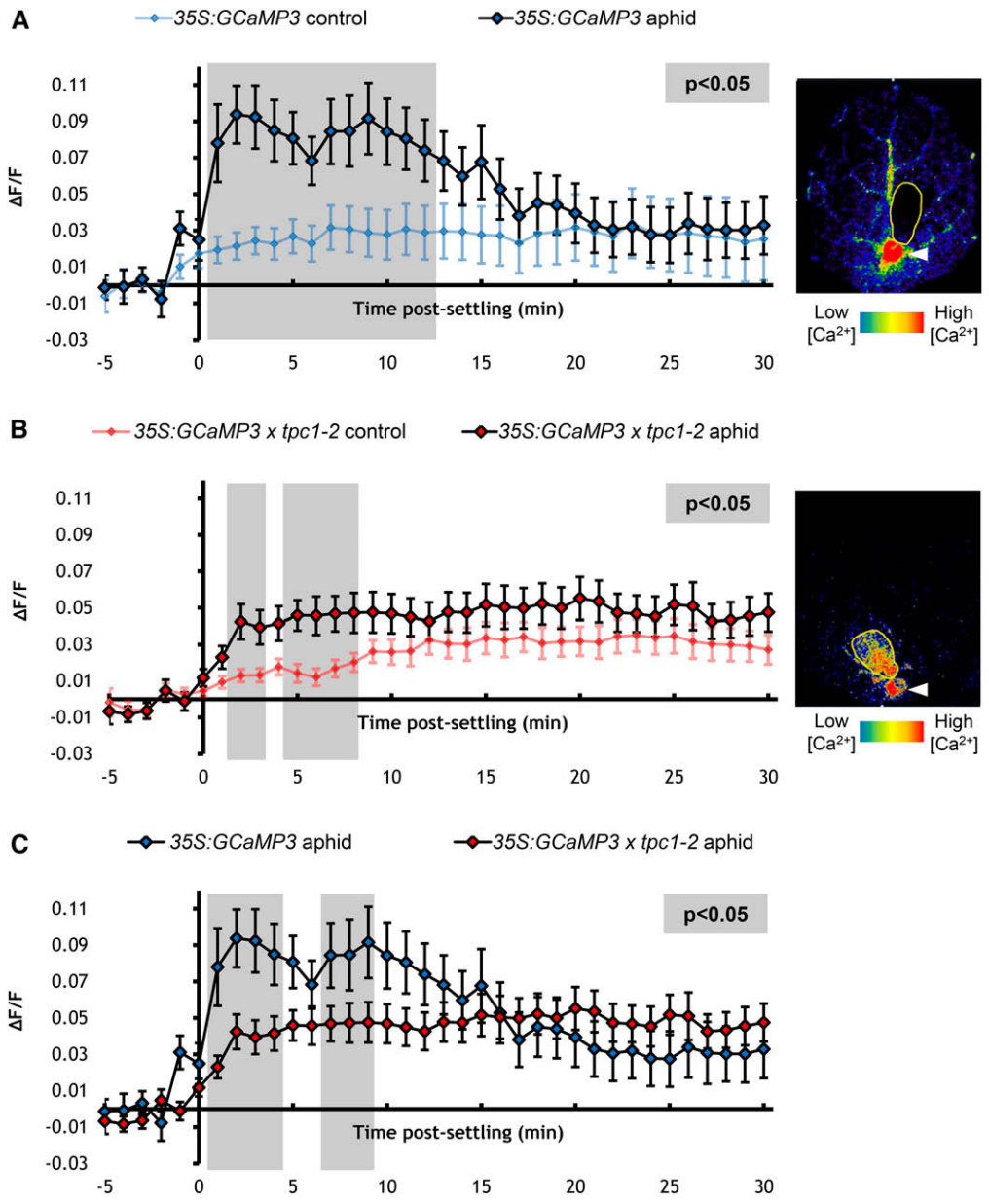

Figure 7. *TPC1* Contributes to Aphid-Elicited $[Ca^{2+}]_{cyt}$ Elevations.

(A) Left: Normalized fluorescence (ΔF/F) around feeding sites of aphid-exposed *35S:GCaMP3* leaves and no-aphid controls. Error bars represent SE of the mean (n = 27). Gray shading indicates significant difference between treatments (Student's t test within GLM at $P < 0.05$). Right: Representative stereomicroscope image of the $[Ca^{2+}]_{cyt}$ elevation seen around a feeding site of a *35S:GCaMP3* leaf. GFP fluorescence is color-coded according to the inset scale. Aphid outlined in yellow and feeding site indicated with an arrowhead. Image taken 1 min after settling.

(B) Left: ΔF/F around feeding sites of aphid-exposed *35S:GCaMP3* × *tpc1-2* leaves and no-aphid controls. Error bars represent SE of the mean (n = 29). Gray shaded areas indicate significant differences between the two treatments (Student's t test within GLM at $P < 0.05$). Right: Representative stereomicroscope image of the reduction in $[Ca^{2+}]_{cyt}$ elevation seen around a feeding site of a *35S:GCaMP3* × *tpc1-2* leaf. GFP fluorescence is color-coded according to the inset scale. Aphid outlined in yellow and feeding site indicated with an arrowhead. Image taken 2 min after settling.

(C) Comparison of ΔF/F around feeding sites of aphid-exposed *35S:GCaMP3* and *35S:GCaMP3* × *tpc1-2* leaves. Data of aphid exposures shown in **(A)** and **(B)** were replotted together. Areas shaded in gray indicate significant differences between the two treatments (Student's t test within GLM at $P < 0.05$).

7B and 7C; Supplemental Movie 7), implying that intracellular Ca^{2+} is involved in the $[Ca^{2+}]_{cyt}$ elevations. Overexpression of *TPC1* had no effect on the initial phases of $[Ca^{2+}]_{cyt}$ elevation, though the elevation was significantly extended beyond 25 min in a non-aphid-specific manner (Figure 8; Supplemental Movie 8).

Overactivation of TPC1 Results in Systemic $[Ca^{2+}]_{cyt}$ Elevations and Decreased Aphid Fecundity

Overactivation of TPC1 can be achieved via the *fatty acid oxygenation upregulated2* (*fou2*) mutation that results in enhanced TPC1 channel opening (Bonaventure et al., 2007a). *35S:GCaMP3* × *fou2* leaves showed unchanged $[Ca^{2+}]_{cyt}$ elevations around *M. persicae* feeding sites (Figure 9A). However, $[Ca^{2+}]_{cyt}$ elevations in leaf tissue systemic to the aphid-feeding sites were detected and these elevations were significantly higher than those observed in *35S:GCaMP3* leaves (Figures 9B and 9C; Supplemental Movie 9).

To determine whether the feeding site $[Ca^{2+}]_{cyt}$ elevation had an effect on aphid fitness, the number of progeny produced by *M. persicae* (fecundity) was assessed. *M. persicae* fecundity was unaltered on the *glr3.3 glr3.6* mutant (Figure 10A) the *tpc1-2* mutant (Figure 10B) and the *35S:TPC1 5.6* line (Figure 10C). *M. persicae* fecundity on the *bak1-5* mutant has been assessed previously and is also not significantly different from the wild type (Prince et al., 2014). However, the *fou2* mutation resulted in a significant reduction in *M. persicae* fecundity (Figure 10D). Interestingly, when the *fou2* mutant was crossed with the jasmonic acid (JA) synthesis mutant *allene oxide synthase* (*aos*) (Park et al., 2002), the *M. persicae* fecundity was similar to that of wild-type plants (Figure 10D), indicating that the documented increase in JA synthesis in the *fou2* mutant (Bonaventure et al., 2007a) is responsible for the decline in *M. persicae* fecundity. Aphid feeding behavior was also assessed using EPG on the *bak1-5*, *tpc1-2*, and *35S:TPC1 5.6* lines (Supplemental Data Set 1), with few differences found between genotypes.

DISCUSSION

To date, the majority of studies dissecting the genetic components involved in plant biotic $[Ca^{2+}]_{cyt}$ elevations have been conducted by application of elicitors to leaf sections, wounding of leaves via tweezers, or application of chewing insects—all treatments that typically involve exposure of large number of cells to elicitation. Here, we elucidated the genetic components involved in $[Ca^{2+}]_{cyt}$ elevations upon plant perception of a piercing-sucking insect that attacks only a small number of epidermal and mesophyll cells within a leaf, as outlined in Figure 11. Aphids trigger $[Ca^{2+}]_{cyt}$ elevations during probing of epidermal and mesophyll cells. These $[Ca^{2+}]_{cyt}$ elevations are dependent on *BAK1* and *GLR3.3*/*GLR3.6*, which are key regulators of PTI and import of extracellular Ca^{2+} into the plant cell cytoplasm, respectively (Chinchilla et al., 2007; Tapken and Hollmann, 2008; Vincill et al., 2012). Furthermore, this study has revealed the role of an endomembrane channel, TPC1, in this interaction and provides evidence for the role of TPC1 in Ca^{2+}-induced Ca^{2+} release (Allen and Sanders, 1996; Ward and Schroeder, 1994). In accordance with this interpretation, $[Ca^{2+}]_{cyt}$ elevations were amplified in the *fou2* mutant, which has an overactive TPC1 channel (Bonaventure et al., 2007a, 2007b), and this resulted in *M. persicae* producing less progeny, implying that TPC1 plays a role in plant immunity.

The dependence of the aphid-elicited $[Ca^{2+}]_{cyt}$ elevation on *BAK1* clearly demonstrates that this response forms part of PTI. While wounding during herbivory by chewing insects is sufficient to induce Ca^{2+} signaling (Maffei et al., 2004; Yang et al., 2012; Kiep et al., 2015), aphids probe only a small number of cells (Will and van Bel, 2006) and thus are more comparable to microbial pathogens. Indeed, *BAK1* is an essential component of PTI against microbial pathogens (Chinchilla et al., 2007; Heese et al., 2007) and aphids (Prince et al., 2014; Chaudhary et al., 2014). Several plasma membrane PRRs that interact with *BAK1* have been implicated in Ca^{2+} release during plant-microbe interactions, including CERK1, FLS2, EFR, and PEPR1 (Miya et al., 2007; Jeworutzki et al., 2010; Qi et al., 2010; Ma et al., 2012). Elicitors that are detected by such PRRs, including chitin, flg22, elf18, and Pep3, all induce rapid $[Ca^{2+}]_{cyt}$ elevations in Arabidopsis leaves within 2 to 3 min (Ranf et al., 2008; Ma et al., 2012; Keinath et al., 2015), comparable to the rapid elevations seen in response to aphid feeding. While GroEL from the aphid endosymbiont *Buchnera aphidicola* has been identified as the aphid elicitor of BAK1-mediated PTI (Chaudhary et al., 2014), CERK1, FLS2, EFR, and PEPR1 are not involved (Prince et al., 2014). Our study provides direct, in vivo evidence of the involvement of BAK1 in PTI $[Ca^{2+}]_{cyt}$ elevations that are unlikely to be the result of wounding and implicates the involvement of an as yet unknown PRR in mediating these elevations.

Plant $[Ca^{2+}]_{cyt}$ elevations are observed in a larger area than the small number of cells directly probed by the aphid stylets (Tjallingii, 1985; Tjallingii and Esch, 1993) and can be detected within 95 s of aphid settling, suggesting that $[Ca^{2+}]_{cyt}$ elevations spread within the epidermal and mesophyll cells upon perception of aphid feeding. However, the highly localized spread of the feeding site $[Ca^{2+}]_{cyt}$ elevation in the epidermal and mesophyll cells is significantly different from the systemic, phloem-based signals seen in response to wounding and herbivory (Mousavi et al., 2013; Kiep et al., 2015). In addition, the 6-μm/s speed of the Ca^{2+} spread is significantly slower than the systemically propagating Ca^{2+} signals in roots during salt stress, or the electrical signals within leaves during wounding, both of which travel at around 400 μm/s (Choi et al., 2014; Mousavi et al., 2013). Indeed, a phloem-based signal is required for systemic spread (Mousavi et al., 2013; Kiep et al., 2015), and this might explain the lack of long-distance systemic $[Ca^{2+}]_{cyt}$ elevations in response to aphids. Agreeing with this, *M. persicae* feeding fails to prime systemic defenses in Arabidopsis (Zhang et al., 2015), unlike microbial pathogens (Traw et al., 2007; Conrath, 2011). This lack of response suggests that the aphid might be actively suppressing systemic signaling, as seen with caterpillars (Kiep et al., 2015). Taken together, our data describe a $[Ca^{2+}]_{cyt}$ elevation that spreads outside of the phloem, in the epidermal and mesophyll cells upon perception of a biotic threat.

GLR3.3 and *GLR 3.6* are also required for the aphid-elicited $[Ca^{2+}]_{cyt}$ elevations to occur, establishing the apoplast as a source of the Ca^{2+} released during detrimental biotic interactions. An influx of Ca^{2+} from the extracellular space can be observed during

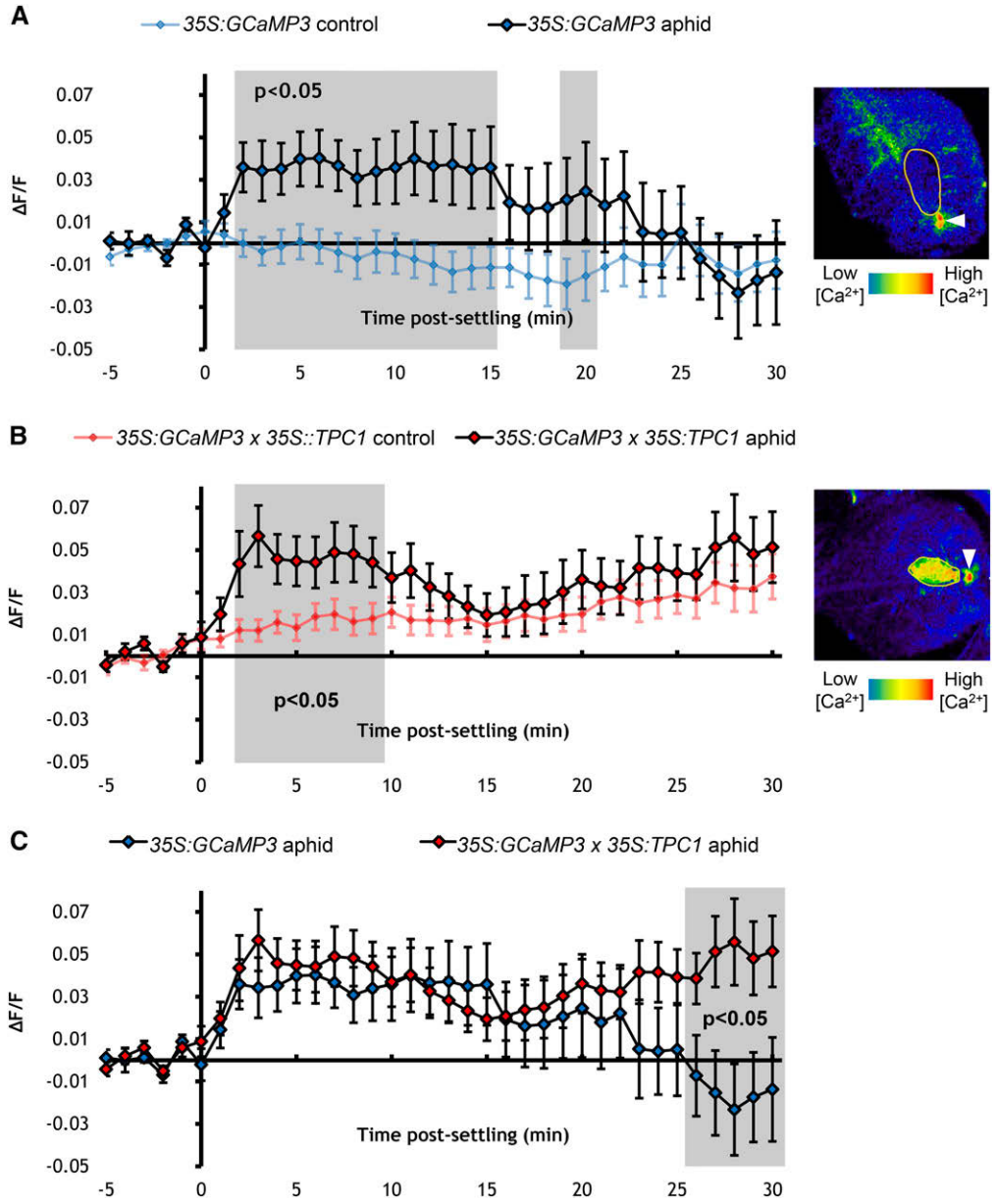

Figure 8. *TPC1* Overexpression Has No Effect on Aphid-Elicited $[Ca^{2+}]_{cyt}$ Elevations.

(A) Left: Normalized fluorescence (ΔF/F) around feeding sites of aphid-exposed *35S:GCaMP3* leaves and no-aphid controls. Error bars represent SE of the mean (n = 30). Gray shading indicates significant difference between treatments (Student's t test within GLM at $P < 0.05$). Right: Representative stereomicroscope image of the $[Ca^{2+}]_{cyt}$ elevation seen around a feeding site of a *35S:GCaMP3* leaf. GFP fluorescence is color-coded according to the inset scale. Aphid outlined in yellow and feeding site indicated with an arrowhead. Image taken 6 min after settling.

(B) Left: ΔF/F around feeding sites of aphid-exposed *35S:GCaMP3* × *35S:TPC1 5.6* leaves and no-aphid controls. Error bars represent SE of the mean (n = 29). Gray shaded areas indicate significant differences between the two treatments (Student's t test within GLM at $P < 0.05$). Right: Representative stereomicroscope of the $[Ca^{2+}]_{cyt}$ elevation seen around a feeding site of a *35S:GCaMP3* × *35S:TPC1 5.6* leaf. GFP fluorescence is color-coded according to the inset scale. Aphid outlined in yellow and feeding site indicated with an arrowhead. Image taken 5 min after settling.

(C) Comparison of ΔF/F around feeding sites of aphid-exposed *35S:GCaMP3* and *35S:GCaMP3* × *35S:TPC1 5.6* leaves. Data of aphid exposures shown in **(A)** and **(B)** were replotted together. Areas shaded in gray indicate significant differences between the two treatments (Student's t test within GLM at $P < 0.05$).

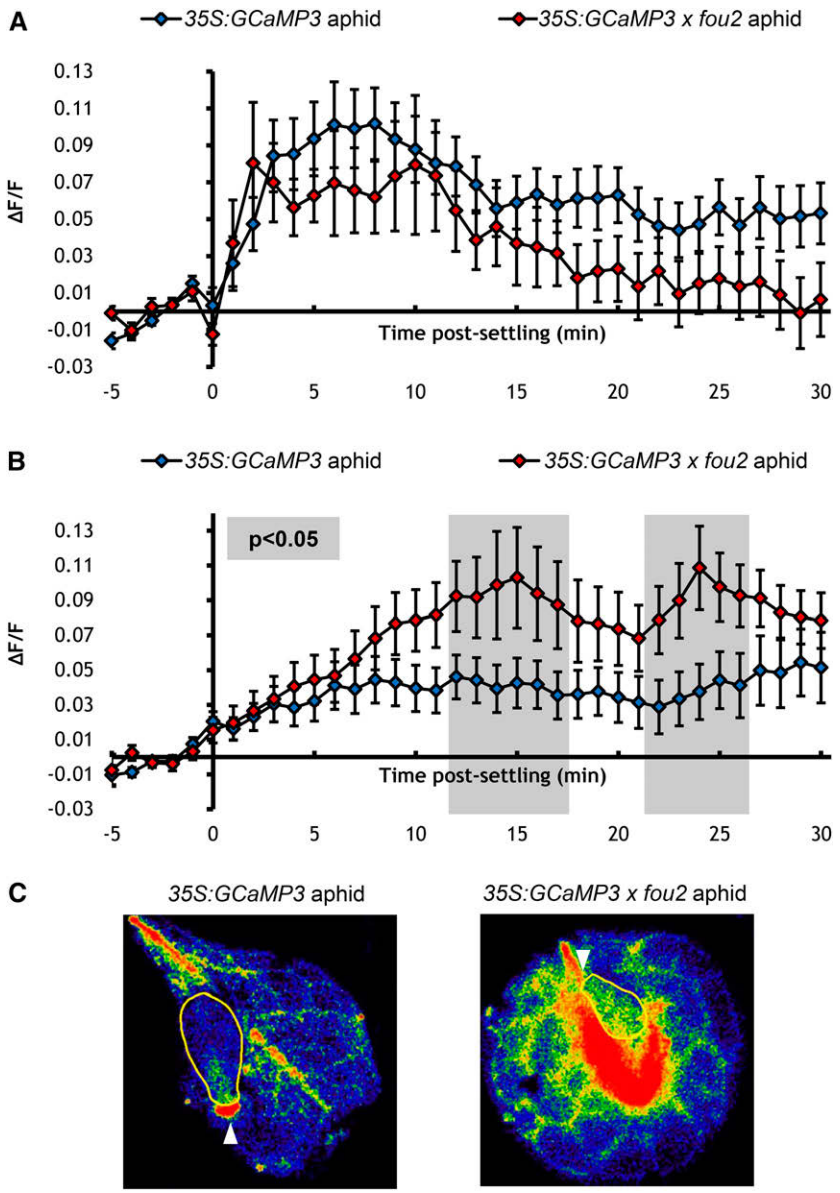

Figure 9. *TPC1* Overactivation (in the *fou2* Mutant) Results in Systemic $[Ca^{2+}]_{cyt}$ Elevations in Response to Aphid Feeding.

(A) Comparison of normalized fluorescence (ΔF/F) around feeding sites of aphid-exposed *35S:GCaMP3* and aphid-exposed *35S:GCaMP3* × *fou2* leaves. Error bars represent SE of the mean (*35S:GCaMP3 n* = 28; *35S:GCaMP3* × *fou2 n* = 25).

(B) Comparison of ΔF/F around systemic lateral tissue sites of aphid-exposed *35S:GCaMP3* and aphid-exposed *35S:GCaMP3* x *fou2* leaves. Error bars represent SE of the mean (*35S:GCaMP3 n* = 28; *35S:GCaMP3* × *fou2 n* = 25). Gray shading indicates significant difference between treatments (Student's *t* test within GLM at $P < 0.05$).

(C) Representative stereomicroscope images of the $[Ca^{2+}]_{cyt}$ elevations seen in *35S:GCaMP3* (left) *35S:GCaMP3* × *fou2* (right) leaves exposed to *M. persicae*. GFP fluorescence is color-coded according to the inset scale. Aphid outlined in yellow and feeding site indicated with an arrowhead. Image on left taken at 2 min after settling; image on right taken at 10 min after settling.

plant-microbe interactions (Gelli et al., 1997; Blume et al., 2000) that can be blocked by plasma membrane channel inhibitors (Zimmermann et al., 1997; Lecourieux et al., 2002, 2005). In addition, a net Ca^{2+} efflux from the extracellular space of tobacco leaf disks was recently measured after *M. persicae* feeding using Ca^{2+}-selective microelectrodes (Ren et al., 2014). *GLR3.3* and *GLR3.6* have been implicated in systemic electrical signaling during wounding (Mousavi et al., 2013; Salvador-Recatalà, 2016), and *GLR3.3* regulates damage perception during oomycete infection (Manzoor et al., 2013). However, given the involvement of *BAK1* in the *M. persicae*-induced $[Ca^{2+}]_{cyt}$ elevation, it is likely that the GLRs are acting as a part of PTI during plant-aphid

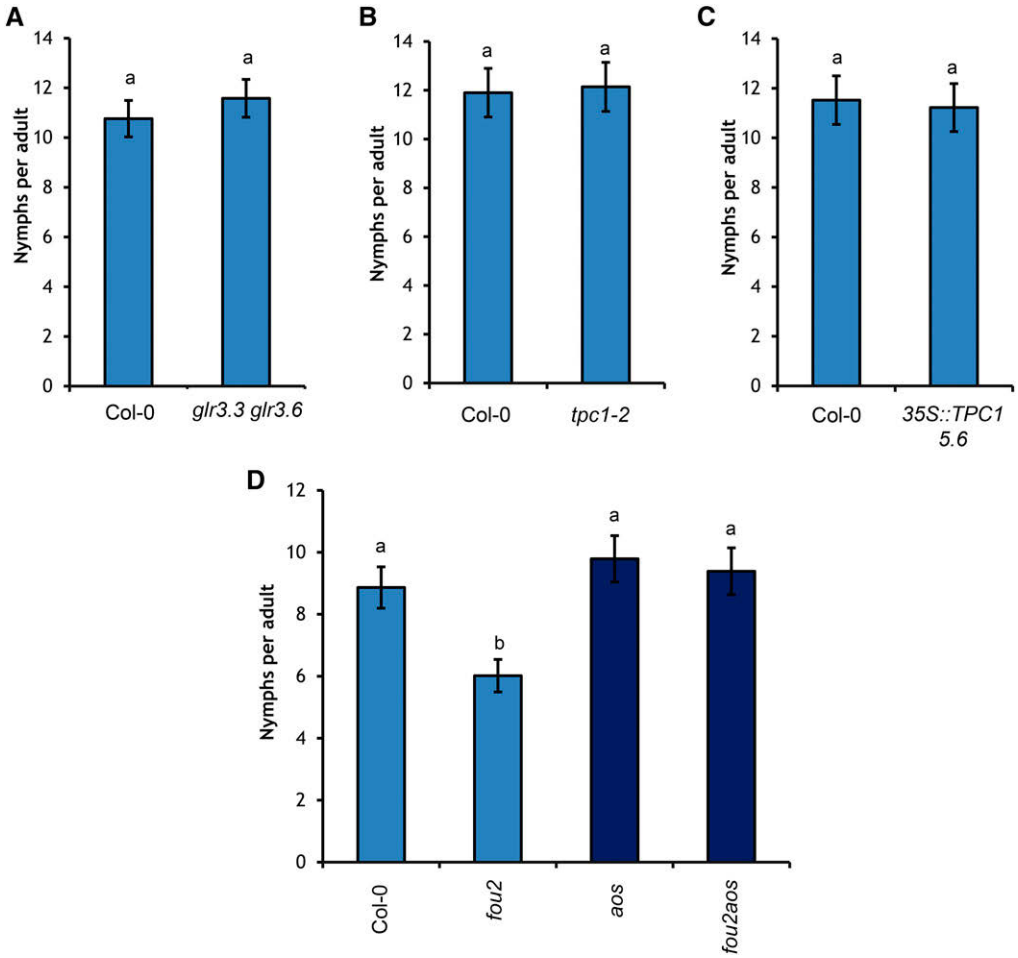

Figure 10. Aphid Fecundity Is Reduced by TPC1 Overactivation (*fou2*), but Not by Altering the Expression of *TPC1* or Abolishing Transcription of *GLR3.3/3.6.*

M. persicae fecundity quantified by the total number of progeny produced per adult over 14 d. Letters indicate significant difference between genotypes (Student's *t* test within GLM, $P < 0.05$).

(A) Fecundity is not altered on the *glr3.3 glr3.6* mutant. Bars represent SE of the mean ($n = 24$).

(B) Fecundity is not altered on the *tpc1-2* mutant. Bars represent SE of the mean ($n = 12$).

(C) Fecundity is not altered on the *35S:TCP1 5.6* line. Bars represent SE of the mean ($n = 12$).

(D) Fecundity is significantly reduced on the *fou2* mutant and can be rescued on the *fou2 aos* double mutant. Bars represent SE of the mean ($n = 16$).

interactions. Indeed, GLRs have been implicated in PAMP perception, with iGluR (mammalian GLR homologs) inhibitors attenuating flg22-, elf18-, and chitin-induced $[Ca^{2+}]_{cyt}$ elevations (Kwaaitaal et al., 2011). Interestingly, it is possible that glutamate itself is a GLR-activating ligand (Chiu et al., 2002; Qi et al., 2006; Forde and Lea, 2007; Stephens et al., 2008). The fungal PAMP cryptogein can elicit an extracellular rise in glutamate and $[Ca^{2+}]_{cyt}$ that is driven by exocytosis (Vatsa et al., 2011), suggesting that glutamate release from the cell is downstream of PAMP perception (Weiland et al., 2016). This might provide a mechanism by which BAK1-mediated glutamate release could stimulate GLR activation. However, to our knowledge, no direct link between BAK1 and glutamate release has yet been established. Our current findings demonstrate a role for the GLRs in local Ca^{2+} signaling and directly identify GLRs as a mechanism leading to of $[Ca^{2+}]_{cyt}$ elevations during biotic interactions.

A long-standing question regarding Ca^{2+} signaling in plants relates to the way in which various Ca^{2+} release pathways interact to produce stimulus-specific signatures. The nature of the interplay of plasma membrane and endomembrane Ca^{2+} release channels has been particularly opaque. It has been hypothesized that *TPC1*, which mediates release of Ca^{2+} from the lumen of the vacuole into the cell cytoplasm (Ward and Schroeder, 1994; Peiter et al., 2005), contributes to Ca^{2+}-induced Ca^{2+} release (Ward and Schroeder, 1994; Allen and Sanders, 1996). Since the feeding site $[Ca^{2+}]_{cyt}$ elevations are attenuated, but not abolished in the *tpc1-2* mutant, it appears that release of vacuolar Ca^{2+} by *TPC1* is downstream of and dependent on extracellular Ca^{2+} release by the GLRs. This finding agrees with work showing that TPC1 activity is

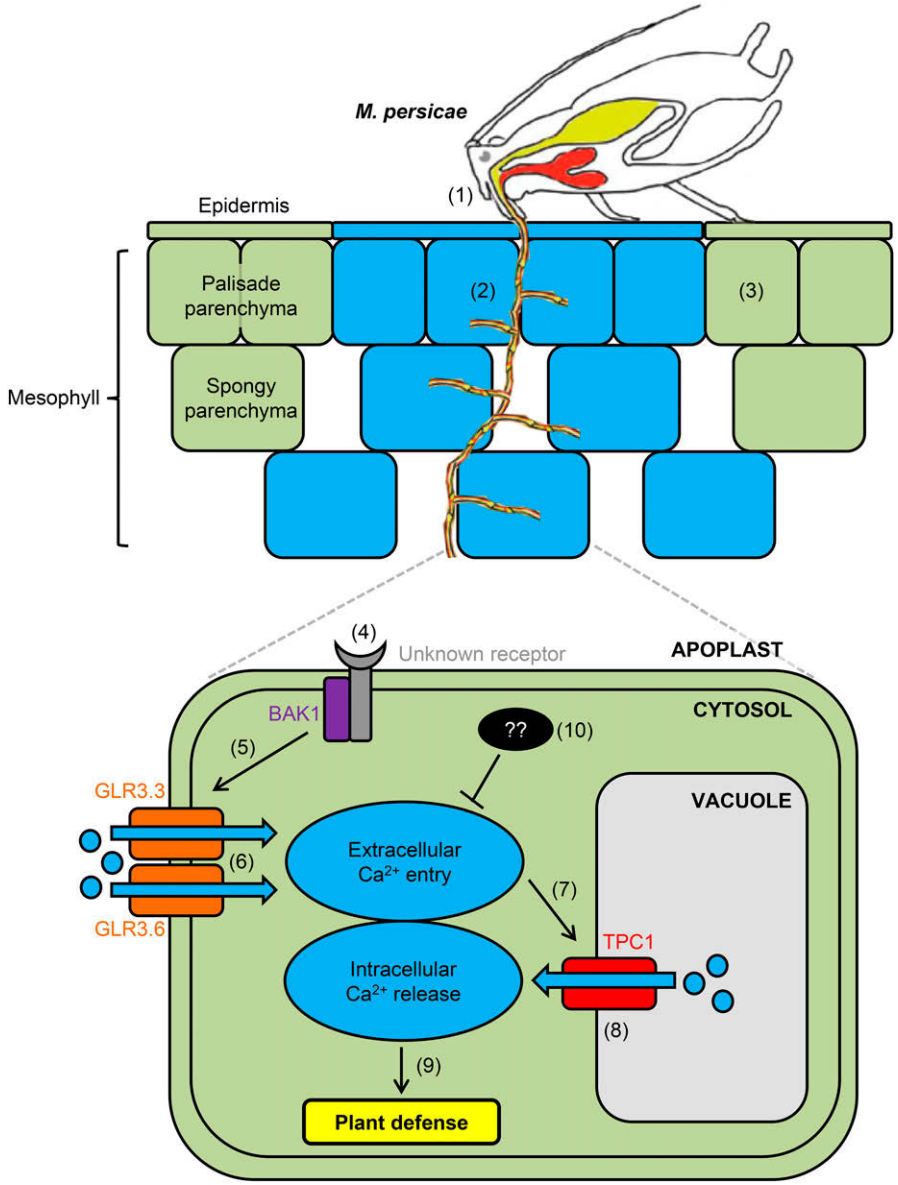

Figure 11. Proposed Model of Ca^{2+} Release during *M. persicae* Feeding.

Aphid image taken from Hogenhout and Bos (2011). (1) Aphids typically probe epidermal and mesophyll cell layers within 31 s of the start of feeding. (2) An aphid-induced $[Ca^{2+}]_{cyt}$ elevation can be detected around the feeding site within 95 s of settling that spreads to adjacent cells. (3) This $[Ca^{2+}]_{cyt}$ elevation is not detected systemically beyond the feeding site. (4) BAK1 and an unknown receptor (PRR) perceive aphid herbivore-associated molecular patterns (HAMPs) (Prince et al., 2014). (5) Perception of aphid HAMPs by BAK1 leads to activation of GLR3.3/GLR3.6, potentially through the release of glutamate (Chiu et al., 2002; Qi et al., 2006; Forde and Lea, 2007; Stephens et al., 2008). (6) GLR3.3/GLR3.6 mediate extracellular Ca^{2+} influx into the cell (Tapken and Hollmann, 2008; Vincill et al., 2012). (7) The increase in $[Ca^{2+}]_{cyt}$ results in activation of TPC1 (Hedrich and Neher, 1987; Ward and Schroeder, 1994). (8) TPC1, either directly or indirectly, mediates release of intracellular Ca^{2+} from the vacuole (Peiter et al., 2005). (9) The increase in $[Ca^{2+}]_{cyt}$ may result in the activation of plant immunity against aphids, which can be enhanced by overactivation of TPC1. (10) During compatible interactions, such as that between Arabidopsis and *M. persicae*, the aphid suppresses plant immunity using effectors (Bos et al., 2010; Mugford et al., 2016), which might also suppress $[Ca^{2+}]_{cyt}$ elevations.

positively regulated by $[Ca^{2+}]_{cyt}$ (Hedrich and Neher, 1987; Ward and Schroeder, 1994; Allen and Sanders, 1996; Guo et al., 2016; Kintzer and Stroud, 2016) and plays a role in systemically propagating Ca^{2+}-induced Ca^{2+} release (Dubiella et al., 2013; Evans et al., 2016; Gilroy et al., 2016; Choi et al., 2016). Consequently, TPC1 appears to be activated by GLR-mediated Ca^{2+} influx and involved in the cell-to-cell spread of Ca^{2+} during biotic interactions. Moreover, mature sieve elements do not contain vacuoles (Esau, 1977), supporting our conclusion that the $[Ca^{2+}]_{cyt}$ elevations do not occur in the phloem, and Arabidopsis spongy

mesophyll cells contain a higher $[Ca^{2+}]_{vac}$ than most other cell types (Conn et al., 2011a, 2011b), making them a significant source of Ca^{2+} influx. Importantly, mesophyll $[Ca^{2+}]_{vac}$ is not significantly altered in *tpc1-2* (Gilliham et al., 2011); consequently, the reduced Ca^{2+} burst in the *tpc1-2* mutant is not related to reduced vacuolar storage of Ca^{2+}. Thus, we identified a role for *TPC1* in Ca^{2+}-induced Ca^{2+} release during biotic interactions, contributing to the growing body of evidence demonstrating the biological relevance of this channel in plants.

Despite the role of *BAK1*, *GLR3.3*, *GLR3.6*, and *TPC1* in generating the aphid-elicited $[Ca^{2+}]_{cyt}$ elevations and the established role of BAK1 and Ca^{2+} in PTI (Blume et al., 2000; Lecourieux et al., 2005; Keinath et al., 2015), abolishing transcription of these genes had no effect on *M. persicae* performance. Downstream of aphid perception by BAK1, hallmarks of PTI such as reactive oxygen species production, callose deposition, and the expression of defense marker genes occur (Prince et al., 2014; Chaudhary et al., 2014). Furthermore, *BAK1* is required for plants to prime defense against *M. persicae* after prior exposure to aphids (Prince et al., 2014). Despite this, *M. persicae* fecundity is unaltered on the *bak1-5* mutant (Prince et al., 2014), as seen for the *glr3.3 glr3.6* or *tpc1-2* mutants in this study. Aphid feeding behavior was also largely unaltered on the *bak1-5* and *tpc1-2* mutants, indicating that the differences in the $[Ca^{2+}]_{cyt}$ elevations observed in these mutants was not the result of altered feeding behavior. We therefore suggest that since *M. persicae* can feed successfully from Arabidopsis, plant immunity is already being sufficiently suppressed. As a result, there is no capacity to increase plant susceptibility to the aphid by disrupting Ca^{2+} signaling. The suppression of Arabidopsis defense by aphids is achieved via effector proteins (Bos et al., 2010; Hogenhout and Bos, 2011; Pitino and Hogenhout, 2013; Atamian et al., 2013; Elzinga et al., 2014; Naessens et al., 2015; Wang et al., 2015; Kettles and Kaloshian, 2016) that are injected into epidermal and mesophyll cells during feeding (Martín et al., 1997; Moreno et al., 2011; Mugford et al., 2016). These effectors may actively suppress the feeding site $[Ca^{2+}]_{cyt}$ elevations, as aphid saliva contains Ca^{2+} binding proteins (Will et al., 2007; Carolan et al., 2009; Rao et al., 2013). Accordingly, the $[Ca^{2+}]_{cyt}$ elevations observed in response to *M. persicae* are not sufficient to activate additional defense, adding to a growing body of evidence showing that this insect is a highly adapted plant pest.

In agreement with the hypothesis that Ca^{2+} signaling forms part of the plant defense response, which *M. persicae* may be suppressing, enhancement of the feeding site $[Ca^{2+}]_{cyt}$ elevations was detrimental to the aphids. Overactivation of *TPC1* via the *fou2* mutation resulted in the generation of systemic $[Ca^{2+}]_{cyt}$ signals not seen in wild-type plants and significantly reduced aphid fecundity. These observations fit with the understanding that TPC1 is regulated posttranscriptionally (Gfeller et al., 2011) and is involved in systemic Ca^{2+} signaling (Choi et al., 2014; Kiep et al., 2015) and that the *fou2* mutation is detrimental to the specialist aphid *Brevicoryne brassicae* (Kuśnierczyk et al., 2011). Given the lack of a phenotype in the *TPC1* overexpression line, these data also imply that the voltage sensitivity of TPC1 is more important than protein abundance in biotic interactions. Furthermore, this result suggests that in vivo there is a role for changes in the transtonoplast voltage to regulate vacuolar Ca^{2+} release and aphid defense responses. The detrimental effect of the *fou2* mutation on *M. persicae* was dependent on JA production by *AOS*, in accordance with the upregulation of JA and JA-related transcripts in the *fou2* mutant (Bonaventure et al., 2007a, 2007b). The involvement of JA in aphid-plant interactions is unclear, with some reporting an effect of JA on aphids (Ellis et al., 2002) and others not (Staswick et al., 1992; Kuśnierczyk et al., 2011; Kettles et al., 2013). Furthermore, the activation of systemic $[Ca^{2+}]_{cyt}$ elevations in the *fou2* mutant suggests that systemic spread of the signal via Ca^{2+}-induced Ca^{2+} release might lead to activation of defense and that aphid suppression of this is based on restricting these signals to a small area. Thus, our data suggest that overactivation of Ca^{2+} signaling is a potential mechanism by which to increase plant resistance to pests.

METHODS

Arabidopsis thaliana Growth

Plants used in the microscopy and single leaf EPG were grown on 100-mm^2-square plastic plates (R and L Slaughter) on quarter-strength Murashige and Skoog medium (recipe: 1.1 g Murashige and Skoog medium, 7.5 g sucrose, 10 g Formedium agar, and 1 liter deionized water) (Murashige and Skoog, 1962) and stratified for 3 d in the dark (8°C). They were then transferred to a controlled environment room (CER) with a 16-h day and 8-h night (90 μmol m^{-2} s^{-1} sodium lamp), at a constant temperature of 23°C. Plants were used in experiments at 16 to 18 d old. Plants for use in fecundity assays and whole-plant EPG were germinated and maintained on Scotts Levington F2 compost. Seeds were stratified for 1 week at 4 to 6°C before being transferred to a CER for 4 to 5 weeks and maintained at 22°C with a photoperiod of 10 h light (90 μmol m^{-2} s^{-1} sodium lamp) and 14 h dark.

Aphids

A stock colony of *Myzus persicae* (clone US1L; Mark Stevens) (Bos et al., 2010) was reared continuously on Chinese cabbage (*Brassica rapa* subsp *chinensis*) in cages in a 16-h-day (90 μmol m^{-2} s^{-1} at 22°C), 8-h-night (20°C) photoperiod. For use in experiments, *M. persicae* individuals of standardized ages were used. These were produced by placing 5 to 15 mixed instar adults from the stock colony onto 4-week-old Arabidopsis (Col-0) grown in a CER with a 16-h-day (90 μmol m^{-2} s^{-1} at 22°C) and 9-h-night (20°C) photoperiod, in pots (13.5-cm diameter, 9-cm depth), and caged inside clear plastic tubing (10 × 15 cm) with a plastic lid. These adults were removed after 24 to 48 h, leaving nymphs of the same age for use in later experiments.

Fluorescence Microscopy

Leaves from plate-grown plants were detached using sharp scissors and placed in the wells of a clear 96-well Microtitre plate (Thermo Fisher Scientific) with 300 μL of distilled water, abaxial surface facing up. These plates were left in the dark at room temperature overnight and used in microscopy the following day. To visualize fluorescence from the *35S:GCaMP3* construct (K_d in vitro = 660 ± 19 nM; Tian et al., 2009), a Leica M205FA stereomicroscope (Leica Microsystems) was used. GFP was excited using a LED light source at 470 nm, and fluorescent emission was captured using a 500- to 550-nm emission filter. Images were captured every 5 s using a Leica DFC310FX camera with a gain of 3.5 and a constant exposure time (1−2.5 s depending on the brightness of the line). The microscope was controlled via Leica Application Suite v3.2.0 (Leica Microsystems). Leaves were imaged in groups of four, two leaves per genotype, at a 7.8× magnification. One 8- to 10-d-old aphid was added to a leaf of each genotype, with the other leaf left uninfested as a control. Each

leaf represented one biological replicate (*n*). Images were captured for 50 to 60 min after aphid application, with the 96-well plate covered in cling film to prevent aphid escape. Images were exported as TIFF files for analysis.

Fluorescent Signal Analysis

TIFF files were imported into Fiji (Image J) v1.48a (National Institutes of Health) and converted into 32-bit images. Fluorescence was analyzed over time for various regions of interest (ROIs) using the Fiji plug-in Time Series Analyzer v2 (University of California, Los Angeles). For aphid treatments, circular ROIs with a 50-pixel (0.65 mm) diameter were selected in three locations: at the feeding site, on the midrib systemic to the aphid-feeding site, and in the tissue beside the midrib (lateral tissue). $\Delta F/F$ was calculated according to the equation $\Delta F/F = (F - F_0)/F_0$, where F_0 was the average baseline fluorescence calculated from the average of F over the first 60 frames of the recording (Keinath et al., 2015) before the aphid settled. Samples in which the controls showed large $[Ca^{2+}]_{cyt}$ elevations ($\Delta F/F > 0.2$) prior to treatment were discarded. The area of the aphid-elicited $[Ca^{2+}]_{cyt}$ elevations was calculated using the Fiji freehand selection tool to draw around the maximum visible GFP signal. For analysis of the speed of the wave front, the Fiji plug-in MTrackJ v 1.5.1 (Meijering et al., 2012) was used. Representative supplemental videos of the aphid-elicited $[Ca^{2+}]_{cyt}$ elevations were created by converting the raw F values to heat maps using the NucMed_Image LUTs plug-in for Fiji (J.A. Parker; www.IEEE.org), with the feeding site Ca^{2+} burst used to determine the color scale. Time information was added using the Time Stamper plug-in (W. Rasband, National Institutes of Health).

Confocal Microscopy

Confocal images of the GCaMP3 signal were acquired with a laser scanning confocal microscope (LSM780/Elyra; Newcomb Imaging Center, Department of Botany, University of Wisconsin, Madison). GCaMP3 was excited by a 488-nm laser, and GFP signal was detected with a 34-element internal GAsP detector.

Crossing Arabidopsis

Crossing was conducted with 4-week-old Arabidopsis plants, grown in a CER at a constant temperature of 22°C with a 16-h-day (HQI lighting)/8-h-night photoperiod. Two unopened buds per stalk were selected, and the remaining buds were removed. The sepals, petals, and stamens were removed from the selected buds, leaving a single carpel. Stamens from the other crossing partner were dissected and pollen transfer between the two was achieved by brushing the stamen against the carpel of the selected mutant. Dissections were performed with a pair of sharp tweezers. Pollinated carpels were covered in 74 × 41-mm paper bags (Global Polythene) sealed with tape and allowed to mature.

Whole-Plant EPG

Experiments were conducted as described previously (Tjallingii, 1978). Adult 13- to 15-d-old *M. persicae* were attached to the Giga-8 EPG system (EPG Systems) using 12.5-μm gold wire (EPG Systems) and silver glue (EPG Systems) and then placed on 4-week old Arabidopsis. One aphid was added to each plant, and this represented one biological replicate (*n*). The experiment was contained inside a Faraday cage to minimize electrical interference. Feeding behavior was recorded for 8 h using Stylet+d (EPG Systems). Each EPG track was then analyzed blind in Stylet+a (EPG Systems). The timing of aphid settling relative to the beginning of probing was also documented. Relevant EPG parameters were calculated using the Microsoft Excel spreadsheet developed by Edgar Schliephake (Julius Kuhn Institute, Germany) (Sarria et al., 2009).

Single-Leaf EPG

Single-leaf EPG was performed using a modified version of the setup described above. Leaves were dissected from plate-grown plants (grown as detailed the microscopy section) and floated in 300 μL of water in 96-well plates. A small piece of copper wire was attached to the EPG ground electrode, and this was inserted into the well. Nine- to eleven-day-old *M. persicae* were then added to these leaves and the experiment was conducted and analyzed as outlined above.

Aphid Fecundity Assay

M. persicae fecundity was assessed as previously described (Pitino et al., 2011). Briefly, five adult aphids from the stock colony were added to each plant at the beginning of the experiment, and after 48 h all adults were removed. After a further 72 h, any excess nymphs were removed, to leave five nymphs per plant. The number of offspring produced by these aphids was counted after 11 and 14 d, as was the final number of adult aphids. Each plant was considered one biological replicate (*n*).

Statistical Analysis

Genstat v18 (VSN International) was used for the majority of statistical analyses. GCaMP3 fluorescence data were assessed using classical linear regression within a general linear model (GLM). Pairwise comparisons between treatments at each time point were conducted within this model using Student's *t* probabilities. Aphid fecundity assays were analyzed by a classical linear regression within a GLM using a Poisson distribution. The model took into account the experimental replicates as an additional factor. Pairwise comparisons between treatments using Student's *t* probabilities were conducted within this model. EPG data were analyzed in R v3.0 (Free Software Foundation) by comparing behaviors between treatments using a Mann-Whitney U test.

Accession Numbers

Sequence data from this article can be found in the Arabidopsis Genome Initiative or GenBank/EMBL databases under the following accession numbers: ADJ53338.1 (GCaMP3), NC_003075.7 (Two-pore channel 1), NC_003075.7 (BRI1-associated receptor kinase), NC_003070.9 (glutamate receptor 3.3), NC_003074.8 (glutamate receptor 3.6), NC_003070.9 (sucrose-proton symporter 2), and NC_003076.8 (allene oxide synthase).

Supplemental Data

Supplemental Figure 1. GCaMP3 subcellular localization in the epidermis of *35S:GCaMP3* leaves, measured by confocal microscopy.

Supplemental Movie 1. The GCaMP3 sensor detects aphid-elicited $[Ca^{2+}]_{cyt}$ elevations in detached leaves.

Supplemental Movie 2. The GCaMP3 sensor detects $[Ca^{2+}]$cyt elevations around the putative aphid-feeding site on leaves of whole Arabidopsis plants.

Supplemental Movie 3. $[Ca^{2+}]_{cyt}$ elevations are detected around feeding sites of aphid-exposed *35S:GCaMP3* leaves, but not *SUC2pro:GCaMP3* leaves.

Supplemental Movie 4. Visualization of $[Ca^{2+}]_{cyt}$ elevations elicited by cold water on *35S:GCaMP3* and *SUC2pro:GCaMP3* leaves.

Supplemental Movie 5. *BAK1* is required for $[Ca^{2+}]_{cyt}$ elevations elicited around aphid-feeding sites.

Supplemental Movie 6. *GLR3.3* and *GLR3.6* are required for $[Ca^{2+}]_{cyt}$ elevations elicited around aphid-feeding sites.

Supplemental Movie 7. *TPC1* contributes to aphid-elicited $[Ca^{2+}]_{cyt}$ elevations.

Supplemental Movie 8. Aphid-induced $[Ca^{2+}]_{cyt}$ elevations are not altered by overexpression of *TPC1*.

Supplemental Movie 9. Overactivation of TPC1 results in systemic aphid-elicited $[Ca^{2+}]_{cyt}$ elevations.

Supplemental Data Set 1. Aphid feeding behaviors analyzed by EPG on selected Arabidopsis mutants (pairwise comparisons).

ACKNOWLEDGMENTS

We thank Grant Calder (John Innes Centre, UK) and W. Fred Tjallingii (EPG Systems, The Netherlands) for their invaluable advice concerning microscopy and EPG, respectively. We also thank Edward Farmer (University of Lausanne, Switzerland) for plant material and the members of the John Innes Centre horticultural and entomology departments for their assistance throughout the project. This work was supported by a PhD studentship from the John Innes Foundation (T.R.V.), by the Biotechnology and Biological Sciences Research Council and the John Innes Foundation (grant B/JJ004561/1) (T.R.V., M.A., J.C., P.H., N.B., S.T.M., M.P., S.A.H., A.J.M., D.S.), by a year in industry placement from the John Innes Centre (M.A.), by a summer studentship from Biochemical Society of the UK (J.C.), JST PRESTO (M.T.), and by National Science Foundation Grants MCB 1329723 and IOS-1557899 (M.T. and S.G.).

AUTHOR CONTRIBUTIONS

T.R.V., S.T.M., A.J.M., S.A.H., and D.S. designed the research. T.R.V., M.A., J.C., P.H., N.B., and M.P. performed experiments. M.T. and S.G. contributed new experimental tools and materials. T.R.V., M.A., J.C., P.H, N.B., and M.P. analyzed results. T.R.V., S.G., A.J.M., S.A.H., and D.S wrote the article.

Received February 21, 2017; revised May 22, 2017; accepted May 29, 2017; published May 30, 2017.

REFERENCES

Aidemark, M., Andersson, C.J., Rasmusson, A.G., and Widell, S. (2009). Regulation of callose synthase activity in situ in alamethicin-permeabilized Arabidopsis and tobacco suspension cells. BMC Plant Biol. **9:** 27.

Allen, G.J., Chu, S.P., Schumacher, K., Shimazaki, C.T., Vafeados, D., Kemper, A., Hawke, S.D., Tallman, G., Tsien, R.Y., Harper, J.F., Chory, J., and Schroeder, J.I. (2000). Alteration of stimulus-specific guard cell calcium oscillations and stomatal closing in Arabidopsis *det3* mutant. Science **289:** 2338–2342.

Allen, G.J., and Sanders, D. (1996). Control of ionic currents in guard cell vacuoles by cytosolic and luminal calcium. Plant J. **10:** 1055–1069.

Atamian, H.S., Chaudhary, R., Cin, V.D., Bao, E., Girke, T., and Kaloshian, I. (2013). *In planta* expression or delivery of potato aphid *Macrosiphum euphorbiae* effectors Me10 and Me23 enhances aphid fecundity. Mol. Plant Microbe Interact. **26:** 67–74.

Blackman, R.L., and Eastop, V.F. (2000). Aphids on the World's Crops: An Identification and Information Guide. (Chichester, UK: John Wiley & Sons).

Blackman, R.L., and Eastop, V.F. (2007). Taxonomic issues. In Aphids as Crop Pests, H.F. Van Emden and R. Harrington, eds (Wallingford, UK: CABI), pp. 1–31.

Blume, B., Nürnberger, T., Nass, N., and Scheel, D. (2000). Receptor-mediated increase in cytoplasmic free calcium required for activation of pathogen defense in parsley. Plant Cell **12:** 1425–1440.

Bonaventure, G., Gfeller, A., Proebsting, W.M., Hörtensteiner, S., Chételat, A., Martinoia, E., and Farmer, E.E. (2007a). A gain-of-function allele of TPC1 activates oxylipin biogenesis after leaf wounding in Arabidopsis. Plant J. **49:** 889–898.

Bonaventure, G., Gfeller, A., Rodríguez, V.M., Armand, F., and Farmer, E.E. (2007b). The *fou2* gain-of-function allele and the wild-type allele of Two Pore Channel 1 contribute to different extents or by different mechanisms to defense gene expression in Arabidopsis. Plant Cell Physiol. **48:** 1775–1789.

Bos, J.I., Prince, D., Pitino, M., Maffei, M.E., Win, J., and Hogenhout, S.A. (2010). A functional genomics approach identifies candidate effectors from the aphid species *Myzus persicae* (green peach aphid). PLoS Genet. **6:** e1001216.

Bricchi, I., Bertea, C.M., Occhipinti, A., Paponov, I.A., and Maffei, M.E. (2012). Dynamics of membrane potential variation and gene expression induced by *Spodoptera littoralis, Myzus persicae*, and *Pseudomonas syringae* in Arabidopsis. PLoS One **7:** e46673.

Carolan, J.C., Fitzroy, C.I.J., Ashton, P.D., Douglas, A.E., and Wilkinson, T.L. (2009). The secreted salivary proteome of the pea aphid *Acyrthosiphon pisum* characterised by mass spectrometry. Proteomics **9:** 2457–2467.

Charpentier, M., Sun, J., Vaz Martins, T., Radhakrishnan, G.V., Findlay, K., Soumpourou, E., Thouin, J., Véry, A.A., Sanders, D., Morris, R.J., and Oldroyd, G.E.D. (2016). Nuclear-localized cyclic nucleotide-gated channels mediate symbiotic calcium oscillations. Science **352:** 1102–1105.

Chaudhary, R., Atamian, H.S., Shen, Z., Briggs, S.P., and Kaloshian, I. (2014). GroEL from the endosymbiont *Buchnera aphidicola* betrays the aphid by triggering plant defense. Proc. Natl. Acad. Sci. USA **111:** 8919–8924.

Chen, J.Q., Rahbe, Y., Delobel, B., Sauvion, N., Guillaud, J., and Febvay, G. (1997). Melon resistance to the aphid *Aphis gossypii*: behavioural analysis and chemical correlations with nitrogenous compounds. Entomol. Exp. Appl. **85:** 33–44.

Chinchilla, D., Bauer, Z., Regenass, M., Boller, T., and Felix, G. (2006). The Arabidopsis receptor kinase FLS2 binds flg22 and determines the specificity of flagellin perception. Plant Cell **18:** 465–476.

Chinchilla, D., Zipfel, C., Robatzek, S., Kemmerling, B., Nürnberger, T., Jones, J.D.G., Felix, G., and Boller, T. (2007). A flagellin-induced complex of the receptor FLS2 and BAK1 initiates plant defence. Nature **448:** 497–500.

Chiu, J.C., Brenner, E.D., DeSalle, R., Nitabach, M.N., Holmes, T.C., and Coruzzi, G.M. (2002). Phylogenetic and expression analysis of the glutamate-receptor-like gene family in *Arabidopsis thaliana.* Mol. Biol. Evol. **19:** 1066–1082.

Choi, W.G., Hilleary, R., Swanson, S.J., Kim, S.H., and Gilroy, S. (2016). Rapid, long-distance electrical and calcium signaling in plants. Annu. Rev. Plant Biol. **67:** 287–307.

Choi, W.G., Toyota, M., Kim, S.H., Hilleary, R., and Gilroy, S. (2014). Salt stress-induced Ca^{2+} waves are associated with rapid, long-distance root-to-shoot signaling in plants. Proc. Natl. Acad. Sci. USA **111:** 6497–6502.

Clough, S.J., Fengler, K.A., Yu, I.C., Lippok, B., Smith, R.K., Jr., and Bent, A.F. (2000). The Arabidopsis *dnd1* "defense, no death" gene encodes a mutated cyclic nucleotide-gated ion channel. Proc. Natl. Acad. Sci. USA **97:** 9323–9328.

Conn, S.J., Conn, V., Tyerman, S.D., Kaiser, B.N., Leigh, R.A., and Gilliham, M. (2011a). Magnesium transporters, MGT2/MRS2-1 and

MGT3/MRS2-5, are important for magnesium partitioning within *Arabidopsis thaliana* mesophyll vacuoles. New Phytol. **190:** 583–594.

Conn, S.J., et al. (2011b). Cell-specific vacuolar calcium storage mediated by CAX1 regulates apoplastic calcium concentration, gas exchange, and plant productivity in Arabidopsis. Plant Cell **23:** 240–257.

Conrath, U. (2011). Molecular aspects of defence priming. Trends Plant Sci. **16:** 524–531.

Dixon, A. (1998). Aphid Ecology: An Optimization Approach. (London: Springer).

Dodd, A.N., Kudla, J., and Sanders, D. (2010). The language of calcium signaling. Annu. Rev. Plant Biol. **61:** 593–620.

Dubiella, U., Seybold, H., Durian, G., Komander, E., Lassig, R., Witte, C.P., Schulze, W.X., and Romeis, T. (2013). Calcium-dependent protein kinase/NADPH oxidase activation circuit is required for rapid defense signal propagation. Proc. Natl. Acad. Sci. USA **110:** 8744–8749.

Ehrhardt, D.W., Wais, R., and Long, S.R. (1996). Calcium spiking in plant root hairs responding to Rhizobium nodulation signals. Cell **85:** 673–681.

Ellis, C., Karafyllidis, I., and Turner, J.G. (2002). Constitutive activation of jasmonate signaling in an Arabidopsis mutant correlates with enhanced resistance to *Erysiphe cichoracearum, Pseudomonas syringae*, and *Myzus persicae.* Mol. Plant Microbe Interact. **15:** 1025–1030.

Elzinga, D.A., De Vos, M., and Jander, G. (2014). Suppression of plant defenses by a *Myzus persicae* (green peach aphid) salivary effector protein. Mol. Plant Microbe Interact. **27:** 747–756.

Esau, K. (1977). Phloem: Anatomy of Seed Plants. (London: John Wiley and Sons).

Evans, M.J., Choi, W.G., Gilroy, S., and Morris, R.J. (2016). A ROS-assisted calcium wave dependent on the AtRBOHD NADPH oxidase and TPC1 cation channel propagates the systemic response to salt stress. Plant Physiol. **171:** 1771–1784.

Forde, B.G., and Lea, P.J. (2007). Glutamate in plants: metabolism, regulation, and signalling. J. Exp. Bot. **58:** 2339–2358.

Foyer, C.H., Verrall, S.R., and Hancock, R.D. (2015). Systematic analysis of phloem-feeding insect-induced transcriptional reprogramming in Arabidopsis highlights common features and reveals distinct responses to specialist and generalist insects. J. Exp. Bot. **66:** 495–512.

Furch, A.C.U., van Bel, A.J.E., Fricker, M.D., Felle, H.H., Fuchs, M., and Hafke, J.B. (2009). Sieve element Ca^{2+} channels as relay stations between remote stimuli and sieve tube occlusion in *Vicia faba.* Plant Cell **21:** 2118–2132.

Galán, J.E., Lara-Tejero, M., Marlovits, T.C., and Wagner, S. (2014). Bacterial type III secretion systems: specialized nanomachines for protein delivery into target cells. Annu. Rev. Microbiol. **68:** 415–438.

Gelli, A., Higgins, V.J., and Blumwald, E. (1997). Activation of plant plasma membrane Ca^{2+}-permeable channels by race-specific fungal elicitors. Plant Physiol. **113:** 269–279.

Gfeller, A., Baerenfaller, K., Loscos, J., Chételat, A., Baginsky, S., and Farmer, E.E. (2011). Jasmonate controls polypeptide patterning in undamaged tissue in wounded Arabidopsis leaves. Plant Physiol. **156:** 1797–1807.

Gilliham, M., Athman, A., Tyerman, S.D., and Conn, S.J. (2011). Cell-specific compartmentation of mineral nutrients is an essential mechanism for optimal plant productivity–another role for TPC1? Plant Signal. Behav. **6:** 1656–1661.

Gilroy, S., Białasek, M., Suzuki, N., Górecka, M., Devireddy, A.R., Karpiński, S., and Mittler, R. (2016). ROS, calcium, and electric signals: key mediators of rapid systemic signaling in plants. Plant Physiol. **171:** 1606–1615.

Gradogna, A., Scholz-Starke, J., Gutla, P.V., and Carpaneto, A. (2009). Fluorescence combined with excised patch: measuring calcium currents in plant cation channels. Plant J. **58:** 175–182.

Guo, J., Zeng, W., Chen, Q., Lee, C., Chen, L., Yang, Y., Cang, C., Ren, D., and Jiang, Y. (2016). Structure of the voltage-gated two-pore channel TPC1 from *Arabidopsis thaliana.* Nature **531:** 196–201.

Guo, J., Zeng, W., and Jiang, Y. (2017). Tuning the ion selectivity of two-pore channels. Proc. Natl. Acad. Sci. USA **114:** 1009–1014.

Hedrich, R., and Neher, E. (1987). Cytoplasmic calcium regulates voltage-dependent ion channels in plant vacuoles. Nature **329:** 833–836.

Heese, A., Hann, D.R., Gimenez-Ibanez, S., Jones, A.M.E., He, K., Li, J., Schroeder, J.I., Peck, S.C., and Rathjen, J.P. (2007). The receptor-like kinase SERK3/BAK1 is a central regulator of innate immunity in plants. Proc. Natl. Acad. Sci. USA **104:** 12217–12222.

Hogenhout, S.A., and Bos, J.I.B. (2011). Effector proteins that modulate plant–insect interactions. Curr. Opin. Plant Biol. **14:** 422–428.

Jaouannet, M., Morris, J.A., Hedley, P.E., and Bos, J.I. (2015). Characterization of arabidopsis transcriptional responses to different aphid species reveals genes that contribute to host susceptibility and non-host resistance. PLoS Pathog. **11:** e1004918.

Jeworutzki, E., Roelfsema, M.R.G., Anschütz, U., Krol, E., Elzenga, J.T.M., Felix, G., Boller, T., Hedrich, R., and Becker, D. (2010). Early signaling through the Arabidopsis pattern recognition receptors FLS2 and EFR involves Ca-associated opening of plasma membrane anion channels. Plant J. **62:** 367–378.

Jones, J.D.G., and Dangl, J.L. (2006). The plant immune system. Nature **444:** 323–329.

Kauss, H., Kohle, H., and Jeblick, W. (1983). Proteolytic activation and stimulation by Ca^{2+} of glucan synthase from soybean cells. FEBS Lett. **158:** 84–88.

Keinath, N.F., Waadt, R., Brugman, R., Schroeder, J.I., Grossmann, G., Schumacher, K., and Krebs, M. (2015). Live cell imaging with R-GECO1 sheds light on flg22- and chitin-induced transient $[Ca^{2+}]_{cyt}$ patterns in Arabidopsis. Mol. Plant **8:** 1188–1200.

Kettles, G.J., Drurey, C., Schoonbeek, H.J., Maule, A.J., and Hogenhout, S.A. (2013). Resistance of *Arabidopsis thaliana* to the green peach aphid, *Myzus persicae*, involves camalexin and is regulated by microRNAs. New Phytol. **198:** 1178–1190.

Kettles, G.J., and Kaloshian, I. (2016). The potato aphid salivary effector Me47 is a glutathione-S-transferase involved in modifying plant responses to aphid infestation. Front. Plant Sci. **7:** 1142.

Kiegle, E., Moore, C.A., Haseloff, J., Tester, M.A., and Knight, M.R. (2000). Cell-type-specific calcium responses to drought, salt and cold in the Arabidopsis root. Plant J. **23:** 267–278.

Kiep, V., Vadassery, J., Lattke, J., Maaß, J.P., Boland, W., Peiter, E., and Mithöfer, A. (2015). Systemic cytosolic $Ca^{(2+)}$ elevation is activated upon wounding and herbivory in Arabidopsis. New Phytol. **207:** 996–1004.

Kintzer, A.F., and Stroud, R.M. (2016). Structure, inhibition and regulation of two-pore channel TPC1 from *Arabidopsis thaliana.* Nature **531:** 258–262.

Knight, H., and Knight, M.R. (2000). Imaging spatial and cellular characteristics of low temperature calcium signature after cold acclimation in Arabidopsis. J. Exp. Bot. **51:** 1679–1686.

Knight, H., Trewavas, A.J., and Knight, M.R. (1996). Cold calcium signaling in Arabidopsis involves two cellular pools and a change in calcium signature after acclimation. Plant Cell **8:** 489–503.

Knight, M.R., Campbell, A.K., Smith, S.M., and Trewavas, A.J. (1991). Transgenic plant aequorin reports the effects of touch and cold-shock and elicitors on cytoplasmic calcium. Nature **352:** 524–526.

Knoblauch, M., Noll, G.A., Müller, T., Prüfer, D., Schneider-Hüther, I., Scharner, D., Van Bel, A.J.E., and Peters, W.S. (2003). ATP-independent contractile proteins from plants. Nat. Mater. **2:** 600–603.

Knoblauch, M., Peters, W.S., Ehlers, K., and van Bel, A.J.E. (2001). Reversible calcium-regulated stopcocks in legume sieve tubes. Plant Cell **13:** 1221–1230.

Kosuta, S., Hazledine, S., Sun, J., Miwa, H., Morris, R.J., Downie, J.A., and Oldroyd, G.E.D. (2008). Differential and chaotic calcium signatures in the symbiosis signaling pathway of legumes. Proc. Natl. Acad. Sci. USA **105:** 9823–9828.

Kuśnierczyk, A., Tran, D.H., Winge, P., Jørstad, T.S., Reese, J.C., Troczyńska, J., and Bones, A.M. (2011). Testing the importance of jasmonate signalling in induction of plant defences upon cabbage aphid (*Brevicoryne brassicae*) attack. BMC Genomics **12:** 423.

Kwaaitaal, M., Huisman, R., Maintz, J., Reinstädler, A., and Panstruga, R. (2011). Ionotropic glutamate receptor (iGluR)-like channels mediate MAMP-induced calcium influx in *Arabidopsis thaliana.* Biochem. J. **440:** 355–365.

Lecourieux, D., Lamotte, O., Bourque, S., Wendehenne, D., Mazars, C., Ranjeva, R., and Pugin, A. (2005). Proteinaceous and oligosaccharidic elicitors induce different calcium signatures in the nucleus of tobacco cells. Cell Calcium **38:** 527–538.

Lecourieux, D., Mazars, C., Pauly, N., Ranjeva, R., and Pugin, A. (2002). Analysis and effects of cytosolic free calcium increases in response to elicitors in *Nicotiana plumbaginifolia* cells. Plant Cell **14:** 2627–2641.

Ma, Y., Walker, R.K., Zhao, Y., and Berkowitz, G.A. (2012). Linking ligand perception by PEPR pattern recognition receptors to cytosolic Ca^{2+} elevation and downstream immune signaling in plants. Proc. Natl. Acad. Sci. USA **109:** 19852–19857.

Maffei, M., Bossi, S., Spiteller, D., Mithöfer, A., and Boland, W. (2004). Effects of feeding *Spodoptera littoralis* on lima bean leaves. I. Membrane potentials, intracellular calcium variations, oral secretions, and regurgitate components. Plant Physiol. **134:** 1752–1762.

Manzoor, H., Kelloniemi, J., Chiltz, A., Wendehenne, D., Pugin, A., Poinssot, B., and Garcia-Brugger, A. (2013). Involvement of the glutamate receptor AtGLR3.3 in plant defense signaling and resistance to *Hyaloperonospora arabidopsidis.* Plant J. **76:** 466–480.

Martín, B., Collar, J.L., Tjallingii, W.F., and Fereres, A. (1997). Intracellular ingestion and salivation by aphids may cause the acquisition and inoculation of non-persistently transmitted plant viruses. J. Gen. Virol. **78:** 2701–2705.

Mathers, T.C., et al. (2017). Rapid transcriptional plasticity of duplicated gene clusters enables a clonally reproducing aphid to colonise diverse plant species. Genome Biol. **18:** 27.

McAinsh, M.R., Webb, A., Taylor, J.E., and Hetherington, A.M. (1995). Stimulus-induced oscillations in guard-cell cytosolic-free calcium. Plant Cell **7:** 1207–1219.

Meijering, E., Dzyubachyk, O., and Smal, I. (2012). Methods for cell and particle tracking. Methods Enzymol. **504:** 183–200.

Mithöfer, A., and Boland, W. (2008). Recognition of herbivory-associated molecular patterns. Plant Physiol. **146:** 825–831.

Miya, A., Albert, P., Shinya, T., Desaki, Y., Ichimura, K., Shirasu, K., Narusaka, Y., Kawakami, N., Kaku, H., and Shibuya, N. (2007). CERK1, a LysM receptor kinase, is essential for chitin elicitor signaling in Arabidopsis. Proc. Natl. Acad. Sci. USA **104:** 19613–19618.

Moreno, A., Garzo, E., Fernandez-Mata, G., Kassem, M., Aranda, M.A., and Fereres, A. (2011). Aphids secrete watery saliva into plant tissues from the onset of stylet penetration. Entomol. Exp. Appl. **139:** 145–153.

Mousavi, S.A., Chauvin, A., Pascaud, F., Kellenberger, S., and Farmer, E.E. (2013). GLUTAMATE RECEPTOR-LIKE genes mediate leaf-to-leaf wound signalling. Nature **500:** 422–426.

Mugford, S.T., Barclay, E., Drurey, C., Findlay, K.C., and Hogenhout, S.A. (2016). An immuno-suppressive aphid saliva protein is delivered into the cytosol of plant mesophyll cells during feeding. Mol. Plant Microbe Interact. **29:** 854–861.

Murashige, T., and Skoog, F. (1962). A revised medium for rapid growth and bio assays with tobacco tissue cultures. Physiol. Plant. **15:** 473–497.

Musser, R.O., Hum-Musser, S.M., Eichenseer, H., Peiffer, M., Ervin, G., Murphy, J.B., and Felton, G.W. (2002). Herbivory: caterpillar saliva beats plant defences. Nature **416:** 599–600.

Naessens, E., Dubreuil, G., Giordanengo, P., Baron, O.L., Minet-Kebdani, N., Keller, H., and Coustau, C. (2015). A secreted MIF cytokine enables aphid feeding and represses plant immune responses. Curr. Biol. **25:** 1898–1903.

Nam, K.J., and Hardie, J. (2012). Host acceptance by aphids: probing and larviposition behaviour of the bird cherry-oat aphid, *Rhopalosiphum padi* on host and non-host plants. J. Insect Physiol. **58:** 660–668.

Park, J.H., Halitschke, R., Kim, H.B., Baldwin, I.T., Feldmann, K.A., and Feyereisen, R. (2002). A knock-out mutation in allene oxide synthase results in male sterility and defective wound signal transduction in Arabidopsis due to a block in jasmonic acid biosynthesis. Plant J. **31:** 1–12.

Peiter, E., Maathuis, F.J.M., Mills, L.N., Knight, H., Pelloux, J., Hetherington, A.M., and Sanders, D. (2005). The vacuolar Ca^{2+}-activated channel TPC1 regulates germination and stomatal movement. Nature **434:** 404–408.

Pitino, M., Coleman, A.D., Maffei, M.E., Ridout, C.J., and Hogenhout, S.A. (2011). Silencing of aphid genes by dsRNA feeding from plants. PLos One **6:** e25709.

Pitino, M., and Hogenhout, S.A. (2013). Aphid protein effectors promote aphid colonization in a plant species-specific manner. Mol. Plant Microbe Interact. **26:** 130–139.

Prince, D.C., Drurey, C., Zipfel, C., and Hogenhout, S.A. (2014). The leucine-rich repeat receptor-like kinase BRASSINOSTEROID INSENSITIVE1-ASSOCIATED KINASE1 and the cytochrome P450 PHYTOALEXIN DEFICIENT3 contribute to innate immunity to aphids in Arabidopsis. Plant Physiol. **164:** 2207–2219.

Qi, Z., Stephens, N.R., and Spalding, E.P. (2006). Calcium entry mediated by GLR3.3, an Arabidopsis glutamate receptor with a broad agonist profile. Plant Physiol. **142:** 963–971.

Qi, Z., Verma, R., Gehring, C., Yamaguchi, Y., Zhao, Y., Ryan, C.A., and Berkowitz, G.A. (2010). Ca^{2+} signaling by plant Arabidopsis thaliana Pep peptides depends on AtPepR1, a receptor with guanylyl cyclase activity, and cGMP-activated Ca^{2+} channels. Proc. Natl. Acad. Sci. USA **107:** 21193–21198.

Ranf, S., Wünnenberg, P., Lee, J., Becker, D., Dunkel, M., Hedrich, R., Scheel, D., and Dietrich, P. (2008). Loss of the vacuolar cation channel, AtTPC1, does not impair Ca^{2+} signals induced by abiotic and biotic stresses. Plant J. **53:** 287–299.

Rao, S.A.K., Carolan, J.C., and Wilkinson, T.L. (2013). Proteomic profiling of cereal aphid saliva reveals both ubiquitous and adaptive secreted proteins. PLos One **8:** e57413.

Ren, G.W., Wang, X.F., Chen, D., Wang, X.W., and Liu, X.D. (2014). Effects of aphids *Myzus persicae* on the changes of Ca^{2+} and H_2O_2 flux and enzyme activities in tobacco. J. Plant Interact. **9:** 883–888.

Salvador-Recatalà, V. (2016). New roles for the GLUTAMATE RECEPTOR-LIKE 3.3, 3.5, and 3.6 genes as on/off switches of wound-induced systemic electrical signals. Plant Signal. Behav. **11:** e1161879.

Salvador-Recatala, V., and Tjallingii, W.F. (2015). A new application of the electrical penetration graph (EPG) for acquiring and measuring electrical signals in phloem sieve elements. J. Vis. Exp. **101:** e52826.

Sarria, E., Cid, M., Garzo, E., and Fereres, A. (2009). Excel workbook for automatic parameter calculation of EPG data. Comput. Electron. Agric. **67:** 35–42.

Sauge, M.H., Kervella, J., and Rahbe, Y. (1998). Probing behaviour of the green peach aphid *Myzus persicae* on resistant Prunus genotypes. Entomol. Exp. Appl. **89:** 223–232.

Schoonhoven, L., Van Loon, J.J.A., and Dicke, M. (2005). Insect–Plant Biology, 2nd ed. (Oxford: Oxford University Press).

Schwessinger, B., Roux, M., Kadota, Y., Ntoukakis, V., Sklenar, J., Jones, A., and Zipfel, C. (2011). Phosphorylation-dependent differential regulation of plant growth, cell death, and innate immunity by the regulatory receptor-like kinase BAK1. PLoS Genet. **7:** e1002046.

Singh, A., and Paolillo, D.J. (1990). Role of calcium in the callose response of self-pollinated brassica stigmas. Am. J. Bot. **77:** 128–133.

Stadler, R., and Sauer, N. (1996). The *Arabidopsis thaliana* AtSUC2 gene is specifically expressed in companion cells. Bot. Acta **109:** 299–306.

Staswick, P.E., Su, W., and Howell, S.H. (1992). Methyl jasmonate inhibition of root growth and induction of a leaf protein are decreased in an *Arabidopsis thaliana* mutant. Proc. Natl. Acad. Sci. USA **89:** 6837–6840.

Stephens, N.R., Qi, Z., and Spalding, E.P. (2008). Glutamate receptor subtypes evidenced by differences in desensitization and dependence on the GLR3.3 and GLR3.4 genes. Plant Physiol. **146:** 529–538.

Tapken, D., and Hollmann, M. (2008). *Arabidopsis thaliana* glutamate receptor ion channel function demonstrated by ion pore transplantation. J. Mol. Biol. **383:** 36–48.

Thor, K., and Peiter, E. (2014). Cytosolic calcium signals elicited by the pathogen-associated molecular pattern flg22 in stomatal guard cells are of an oscillatory nature. New Phytol. **204:** 873–881.

Tian, L., et al. (2009). Imaging neural activity in worms, flies and mice with improved GCaMP calcium indicators. Nat. Methods **6:** 875–881.

Tjallingii, W.F. (1978). Mechanoreceptors of the aphid labium. Entomol. Exp. Appl. **24:** 731.

Tjallingii, W.F. (1985). lectrical nature of recorded signals during stylet penetration by aphids. Entomol. Exp. Appl. **38:** 177–186.

Tjallingii, W.F., and Esch, T.H. (1993). Fine-structure of aphid stylet routes in plant-tissues in correlation with EPG signals. Physiol. Entomol. **18:** 317–328.

Traw, M.B., Kniskern, J.M., and Bergelson, J. (2007). SAR increases fitness of *Arabidopsis thaliana* in the presence of natural bacterial pathogens. Evolution **61:** 2444–2449.

Vatsa, P., Chiltz, A., Bourque, S., Wendehenne, D., Garcia-Brugger, A., and Pugin, A. (2011). Involvement of putative glutamate receptors in plant defence signaling and NO production. Biochimie **93:** 2095–2101.

Verrillo, F., Occhipinti, A., Kanchiswamy, C.N., and Maffei, M.E. (2014). Quantitative analysis of herbivore-induced cytosolic calcium by using a Cameleon (YC 3.6) calcium sensor in *Arabidopsis thaliana.* J. Plant Physiol. **171:** 136–139.

Vincill, E.D., Bieck, A.M., and Spalding, E.P. (2012). $Ca^{(2+)}$ conduction by an amino acid-gated ion channel related to glutamate receptors. Plant Physiol. **159:** 40–46.

Wang, Y., Kang, Y., Ma, C., Miao, R., Wu, C., Long, Y., Ge, T., Wu, Z., Hou, X., Zhang, J., and Qi, Z. (2017). CNGC2 is a Ca^{2+} influx channel that prevents accumulation of apoplastic Ca^{2+} in the leaf. Plant Physiol. **173:** 1342–1354.

Wang, W., et al. (2015). Armet is an effector protein mediating aphid-plant interactions. FASEB J. **29:** 2032–2045.

Ward, J.M., and Schroeder, J.I. (1994). Calcium-activated K^+ channels and calcium-induced calcium-release by slow vacuolar ion channels in guard-cell vacuoles implicated in the control of stomatal closure. Plant Cell **6:** 669–683.

Weiland, M., Mancuso, S., and Baluska, F. (2016). Signalling via glutamate and GLRs in *Arabidopsis thaliana.* Funct. Plant Biol. **43:** 1–25.

Will, T., Tjallingii, W.F., Thönnessen, A., and van Bel, A.J.E. (2007). Molecular sabotage of plant defense by aphid saliva. Proc. Natl. Acad. Sci. USA **104:** 10536–10541.

Will, T., and van Bel, A.J.E. (2006). Physical and chemical interactions between aphids and plants. J. Exp. Bot. **57:** 729–737.

Xiong, T.C., Ronzier, E., Sanchez, F., Corratgé-Faillie, C., Mazars, C., and Thibaud, J.B. (2014). Imaging long distance propagating calcium signals in intact plant leaves with the BRET-based GFP-aequorin reporter. Front. Plant Sci. **5:** 43.

Yamaguchi, Y., Pearce, G., and Ryan, C.A. (2006). The cell surface leucine-rich repeat receptor for AtPep1, an endogenous peptide elicitor in Arabidopsis, is functional in transgenic tobacco cells. Proc. Natl. Acad. Sci. USA **103:** 10104–10109.

Yang, D.H., Hettenhausen, C., Baldwin, I.T., and Wu, J. (2012). Silencing *Nicotiana attenuata* calcium-dependent protein kinases, CDPK4 and CDPK5, strongly up-regulates wound- and herbivory-induced jasmonic acid accumulations. Plant Physiol. **159:** 1591–1607.

Yu, I.C., Parker, J., and Bent, A.F. (1998). Gene-for-gene disease resistance without the hypersensitive response in Arabidopsis *dnd1* mutant. Proc. Natl. Acad. Sci. USA **95:** 7819–7824.

Zhang, X., Xue, M., and Zhao, H.P. (2015). Species-specific effects on salicylic acid content and subsequent *Myzus persicae* (Sulzer) performance by three phloem-sucking insects infesting *Nicotiana tabacum L.* Arthropod-Plant Interact. **9:** 383–391.

Zhu, X., Caplan, J., Mamillapalli, P., Czymmek, K., and Dinesh-Kumar, S.P. (2010). Function of endoplasmic reticulum calcium ATPase in innate immunity-mediated programmed cell death. EMBO J. **29:** 1007–1018.

Zimmermann, S., Nürnberger, T., Frachisse, J.M., Wirtz, W., Guern, J., Hedrich, R., and Scheel, D. (1997). Receptor-mediated activation of a plant Ca^{2+}-permeable ion channel involved in pathogen defense. Proc. Natl. Acad. Sci. USA **94:** 2751–2755.

Zipfel, C. (2009). Early molecular events in PAMP-triggered immunity. Curr. Opin. Plant Biol. **12:** 414–420.

Zipfel, C., Kunze, G., Chinchilla, D., Caniard, A., Jones, J.D.G., Boller, T., and Felix, G. (2006). Perception of the bacterial PAMP EF-Tu by the receptor EFR restricts Agrobacterium-mediated transformation. Cell **125:** 749–760.